


RESEARCH ARTICLE

A 247-year tree-ring reconstruction of spring temperature and relation to spring flooding in eastern boreal Canada

Alexandre Florent Nolin^{1,2,3}  | Martin Philippe Girardin^{3,4} | Jacques Clément Tardif^{2,3} | Xiao Jing Guo⁴ | France Conciatori² | Yves Bergeron^{1,3}

¹Institut de Recherche sur les Forêts, Université du Québec en Abitibi-Témiscamingue (UQAT), Rouyn-Noranda, Québec, Canada

²Centre for Forest Interdisciplinary Research (C-FIR), University of Winnipeg, Department of Biology/Environmental Studies & Sciences, Winnipeg, Manitoba, Canada

³Centre d'Étude de la Forêt, Université du Québec à Montréal (UQAM), Montréal, Québec, Canada

⁴Natural Resources Canada, Canadian Forest Service, Laurentian Forestry Centre, Sainte-Foy, Québec, Canada

Correspondence

Alexandre Florent Nolin, Institut de Recherche sur les Forêts, Université du Québec en Abitibi-Témiscamingue (UQAT), Rouyn-Noranda, QC J9X 5E4, Canada.

Email: alexandreflorent.nolin@uqat.ca

Funding information

Natural Sciences and Engineering Research Council of Canada Collaborative Research program; RIISQ - Intersectorial Flood Network of Québec (2nd program 2020–2021)

Abstract

Few records of spring paleoclimate are available for boreal Canada, as biological proxies recording the beginning of the warm season are uncommon. Given the spring warming observed during the last decades, and its impact on snow-melt and hydrological processes, searching for spring climate proxies is receiving increasing attention. Tree-ring anatomical features and intra-annual widths were used to reconstruct the regional March to May mean air temperature from 1770 to 2016 in eastern boreal Canada. Nested principal component regressions calibrated on 116 years of gridded temperature data were developed from one *Fraxinus nigra* and 10 *Pinus banksiana* sites. The reconstruction indicated three distinct phases in spring temperature variability since 1770. Ample phases of multi-decadal warm and cold springs persisted until the end of the Little Ice Age (1850–1870 CE) and were gradually replaced since the 1940s by decadal to interannual variability associated with an increase in the frequency and magnitude of warm springs. Significant correlations with other paleotemperature records, gridded snow cover extent and runoff support that historical high flooding were associated with late, cold springs with heavy snow cover. Most of the high magnitude spring floods reconstructed for the nearby Harricana River also coincided with the lowest reconstructed spring temperature per decade. However, the last 40 years of observed and reconstructed mean spring temperature showed a reduction in the number of extreme cold springs contrasting with the last few decades of extreme flooding in the eastern Canadian boreal region. This result indicates that warmer late spring mean temperatures on average may contribute, among other factors, to advance the spring break-up and to likely shift the contribution of snow to rain in spring flooding processes.

KEYWORDS

climate change, dendroclimatic reconstruction, *Fraxinus nigra*, generalized additive mixed models (GAMM), *Pinus banksiana*, spring temperature

This is an open access article under the terms of the Creative Commons Attribution-NonCommercial-NoDerivs License, which permits use and distribution in any medium, provided the original work is properly cited, the use is non-commercial and no modifications or adaptations are made.

© 2022 The Authors. *International Journal of Climatology* published by John Wiley & Sons Ltd on behalf of Royal Meteorological Society.

1 | INTRODUCTION

Boreal territories are prone to the impacts of climate warming given the importance of snow accumulation and snowmelt in their hydrological cycle (Buttle *et al.*, 2016; Aygün *et al.*, 2019). In northern Canada, and particularly since 1948, annual average temperature has increased three times faster ($+2.3^{\circ}\text{C}$) than the Earth's global rate (Bush and Lemmen, 2019). The greatest observed warming occurred in winter and spring months resulting in a significant decrease in the length of the ice season (Bush and Lemmen, 2019). Spring snowmelt and ice break-up have occurred earlier since the beginning of the 20th century and this trend has been consistent across Canada (Zhang *et al.*, 2001a; Burn and Elnur, 2002; Prose and Bonsal, 2004; Duguay *et al.*, 2006; Cunderlik and Ouarda, 2009; Déry *et al.*, 2009; Fu and Yao, 2015; Jones *et al.*, 2015; Vincent *et al.*, 2015; Aygün *et al.*, 2019; Chen and She, 2020). Similarly, and since the 1950s, monthly mean discharge across Canada has shown significant increases in March and April, and significant decreases in May (Zhang *et al.*, 2001a). The timing of river and lake ice break-up has also been found to be significantly and negatively correlated with spring air temperature across Canada (Duguay *et al.*, 2006; Fu and Yao, 2015; Chen and She, 2020). As a result, snow cover extent and duration declined and particularly in the eastern part of the country (Brown, 2010; Mudryk *et al.*, 2018; Aygün *et al.*, 2019). Snow water equivalent (SWE) has generally declined in Canada since the 1950s except in northern and central Québec where it has increased (Brown, 2010; Aygün *et al.*, 2019). In this region, increased mid-winter thaw, winter rainfall instead of snow, and rain-on-snow events (Brown, 2010; Jeong and Sushama, 2018; Vincent *et al.*, 2018) may also contribute to increase the SWE by ice layering, and thus the water available for spring runoff from snowmelt. Increasing air temperatures increase the rate of evaporation and atmospheric humidity, which is particularly noticeable in winter at high latitudes because total precipitation (snow and rain) is normally limited by below-freezing temperatures and low atmospheric humidity (Davis *et al.*, 1999; Zhang *et al.*, 2000). The warming of northern and eastern Canada since 1900 was then associated with an increase in the number of heavy rainfall events in spring and in the number of heavy snowfall events in autumn and winter (Zhang *et al.*, 2001b). Warm extremes are also becoming warmer and more frequent, while cold extremes are becoming less cold and less frequent, particularly in northern Canada and since the 1950s (Vincent *et al.*, 2018; Wan *et al.*, 2019).

Trend analyses in flood frequency and magnitude in northeastern Canada consequently demonstrated that spring flooding has increased during the 20th and 21st

centuries (Burn and Whitfield, 2016, 2017; Buttle *et al.*, 2016; Bush and Lemmen, 2019; Nolin *et al.*, 2021b). In the Lake Duparquet area (northwestern Québec) the frequency and magnitude of spring flooding increased since 1850–1870 (Tardif and Bergeron, 1997; Nolin *et al.*, 2021b) which correspond to the end of the Little Ice Age in northeastern Canada (Viau and Gajewski, 2009). Particularly since the last century (1900–2016), high spring discharges therein have been positively associated to cold and early winter and to cold and late spring with a persistent snowpack (Nolin *et al.*, 2021b). However, an increase in the rainfall-to-total-precipitation ratio during the spring–summer season in the Arctic (1979–2015; Han *et al.*, 2018) suggests that the increase in snowfall currently observed in northeastern Canada might be transitory. Climate change scenarios for northern Canada project a 2–17% increase in total precipitation by 2100, with a shift from snow to rain in the spring and fall (Bush and Lemmen, 2019).

Future climate projections for Canada consider multiple possible regional changes in mean air temperature, with low emissions scenarios projecting a $+2.0^{\circ}\text{C}$ increase and high emissions scenarios projecting a $+6.0^{\circ}\text{C}$ increase by 2100 (Bush and Lemmen, 2019). Climate change scenarios indicate an increase in flood risk over northern Canada and a decrease in flood risk over northeastern Québec (Gaur *et al.*, 2018). Snow cover projections point towards a general decrease in snow accumulation in winter (Mudryk *et al.*, 2018) and towards a quicker spring snowmelt over the next hundred years (Minville *et al.*, 2008). Regional climate model projections for northern Québec and Ontario consequently indicate that rain may contribute more to seasonal discharge in winter by 2050 compared to the 20th century (Guay *et al.*, 2015; Wang *et al.*, 2015; Clavet-Gaumont *et al.*, 2017).

The 20th century warming trend associated with anthropogenic activities (Bush and Lemmen, 2019) is now superimposed to the natural internal climate variability (Vincent *et al.*, 2015; Wan *et al.*, 2019). Knowledge of this natural variability remains dependent on instrumental and observational data, but the availability of climate and hydrological data is poor in northeastern Canada, with very few records predating the 1950s (Mortsch *et al.*, 2015; Bush and Lemmen, 2019; Nolin *et al.*, 2021a). Analyses of past variability in spring flood risk and projected hydroclimatic changes remain limited (Mortsch *et al.*, 2015; Buttle *et al.*, 2016; Gaur *et al.*, 2018; Nolin *et al.*, 2021b). In addition, given that most of Canada's electricity generation relies on hydropower plants located in the north (Cherry *et al.*, 2017), understanding natural hydroclimatic variability and placing ongoing hydroclimatic changes in a historical

context is crucial for flood risk management (Ashmore and Church, 2001; Boucher *et al.*, 2011; Bush and Lemmen, 2019).

Tree rings have proven to be one of the most versatile proxy for studying climate variations on the scale of the last centuries to millennia and various tree-ring records have been developed to reconstruct precipitation (Griffin *et al.*, 2013), temperature (Jacoby *et al.*, 1988; Girardin *et al.*, 2009; Tardif *et al.*, 2011), snowpack (Mood *et al.*, 2020; Shamir *et al.*, 2020; Touchan *et al.*, 2021), or extreme events such as droughts (Girardin *et al.*, 2006; Hoffer and Tardif, 2009) and floods (Boucher *et al.*, 2011; Ballesteros-Cánovas *et al.*, 2020; Nolin *et al.*, 2021b). Across northern North America, temperature reconstructions have been successfully derived from annual tree-ring widths (Jacoby and D'Arrigo, 1989) and/or maximum latewood density data (Briffa *et al.*, 1994; 2001; Davi *et al.*, 2003; Youngblut and Luckman, 2008; Anchukaitis *et al.*, 2013; Gennaretti *et al.*, 2014) as well as its surrogate blue intensity (Wilson *et al.*, 2014) or in use with combination of stable isotopes (Barber *et al.*, 2004; Gennaretti *et al.*, 2017). Light rings were also successfully used to reconstruct summer temperatures in Interior North America (Girardin *et al.*, 2009; Tardif *et al.*, 2011). In the boreal region, tree-ring records are obviously biased towards the active growing season and most of the reconstructions (*Alaska and Yukon*: Davi *et al.*, 2003; Barber *et al.*, 2004; Youngblut and Luckman, 2008; Anchukaitis *et al.*, 2013; *northern North America*: Briffa *et al.*, 1994; *Interior North America*: Girardin *et al.*, 2009; Tardif *et al.*, 2011; *northern Québec*: Jacoby *et al.*, 1988; Gennaretti *et al.*, 2014; 2017; *Fennoscandia*: Briffa *et al.*, 1988) have focused on the maximum temperature of the warm season or summer temperature with very few attempts to reconstruct spring or winter temperature variability from tree rings (Guiot, 1987).

As the largest temperature changes reported by instrumental records since the early 20th century in northern Canada occur during the ice season (Aygün *et al.*, 2019; Bush and Lemmen, 2019), it is important to develop temperature reconstructions for winter and spring. Chronologies developed from intra-annual tree-ring widths may contain such climate signals compared to those of annual tree-rings. Total tree-ring widths integrate climate signals over several months during the preceding and current growing seasons, while earlywood (EW) and latewood (LW) width may integrate climate during the season of their formation (Tardif, 1996; Meko and Baisan, 2001; Therrell *et al.*, 2002; Stahle *et al.*, 2009). In coniferous tree species and across the Northern Hemisphere, the EW tends to correlate with climate during the months prior to or during the beginning of the growing season (late winter to early spring) while the LW tends to

correlate with climate during the late growing season (late spring to summer; Fritts, 1976; Meko and Baisan, 2001; Therrell *et al.*, 2002; Stahle *et al.*, 2009; Hoffer and Tardif, 2009; Griffin *et al.*, 2013). Functional dependencies between the formation of EW and LW tissues are also involved. The formation of EW depends on carbohydrates synthesized during the previous growing season and accounts for most of the ring width and hydraulic conductivity, while the formation of LW depends on photoassimilates synthesized during the current growing season (Kozłowski and Pallardy, 1997; Rossi *et al.*, 2013). The inter-correlation between EW and LW can be assessed by removing the linear dependency of the LW width on the preceding EW width using simple linear regression (Meko and Baisan, 2001; Therrell *et al.*, 2002; Griffin *et al.*, 2011) or allometric equation based on the number of tracheids formed during the growing season (Camarero *et al.*, 2021). Seasonal climate forcing on EW and LW production may, nonetheless, be site and species specific. For example, in boreal Sweden EW and LW growth of Scots pine (*Pinus sylvestris* L.) responded positively to spring temperature, although there was a higher correlation between EW width and May temperature (Miina, 2000). Therrell *et al.* (2002) showed that LW chronologies of Douglas fir (*Pseudotsuga menziesii* Franco.) from northern New Mexico responded positively to summer precipitation while LW chronologies from southern New Mexico responded positively to spring precipitation. In central Canada, only the LW chronology responded positively to mean temperature from April to May in jack pine (*Pinus banksiana* Lamb.) while the EW and LW chronologies of black spruce (*Picea mariana* Mill.) responded negatively to early summer temperature (July and July–August respectively; Hoffer and Tardif, 2009).

Dendroclimatic analyses of black ash (*Fraxinus nigra* Marsh.) and jack pine (*P. banksiana* Lamb.) trees conducted over eastern and central boreal Canada demonstrated consistent growth responses to spring climate (Hofgaard *et al.*, 1999; Tardif and Bergeron, 1999; Tardif *et al.*, 2001; Girardin and Tardif, 2005; Girardin *et al.*, 2006; Huang *et al.*, 2010; Genries *et al.*, 2012; Kames *et al.*, 2016). At Lake Duparquet, a warm beginning of the growing season (March–April) negatively affected the number of EW vessels of floodplain *F. nigra* and positively influenced their mean cross-sectional area (Kames *et al.*, 2016), while a warm early summer (May–June) negatively affected radial growth (Tardif *et al.*, 2001). Warm and early spring (March–April) temperatures also favoured the radial growth of *P. banksiana* (Hofgaard *et al.*, 1999; Tardif *et al.*, 2001; Girardin and Tardif, 2005; Girardin *et al.*, 2006; Hoffer and Tardif, 2009; Huang *et al.*, 2010; Genries *et al.*, 2012).

The formation of light-coloured latewood (so called “light ring”) in *P. banksiana* was moreover correlated to the effect of late winter snowfall and cool early springs delaying the onset of cambial activity at the beginning of the growing season (Girardin *et al.*, 2009; Tardif *et al.*, 2011). It can thus be hypothesized that chronologies of intra-annual tree-ring widths of *P. banksiana* and of EW vessels of *F. nigra* trees may contain specific climatic signals related to spring temperature variability, making them suitable candidate tree species for spring temperature reconstruction.

The objectives of this study were threefold: (a) to develop a network of spring-temperature sensitive tree-ring chronologies in eastern boreal Canada from *P. banksiana* and *F. nigra* trees; (b) to reconstruct and assess the variability of spring temperatures for the last 250 years; and (c) to investigate the associations between variations in spring temperature and the recent trends in regional spring flooding since the end of the Little Ice Age.

2 | MATERIAL AND METHODS

2.1 | Study area

The study area encompasses a longitudinal gradient within the northern clay belt of Québec and Ontario near Lake Duparquet, and at the southern fringe of the boreal forest (Figure 1). The region is defined by the

glaciolacustrine flat sediment deposits composing its soils and resulting from the drainage of the proglacial lakes Barlow and Ojibway during the last deglaciation (Daubois *et al.*, 2015). The sub-boreal climate of the area is characterized by a near freezing mean annual air temperature (0.7°C), a high summer humidity (mean annual precipitation of 890 mm), and a considerable amount of snowfall in fall to spring (mean annual snowfall of 250 mm) as indicated for the period 1971–2000 by climate normals from ‘La Sarre’ weather station (48°48′N, 79°1′W; Canadian Climate Normals, http://climate.weather.gc.ca/climate_normals; Figure 1).

Fire is the main natural disturbance in the study area. Post-fire forests are dominated by *P. banksiana* on nutrient-poor and sandy soils, or in associations with paper birch (*Betula papyrifera* Marsh.) and trembling aspen (*Populus tremuloides* Michx.) in more mesic conditions (Bergeron and Dansereau, 1993). After 80–100 years after a fire, forest stands transit towards an association of balsam fir (*Abies balsamea* (L.) Mill.), black spruce, and white spruce (*Picea glauca* (Moench) Voss) (Cayford and McRae, 1983; Bergeron, 2000). Old-growth *F. nigra* forests grow on the lowland floodplains and in association with trembling aspen and eastern white cedar (*Thuja occidentalis* L.) (Tardif and Bergeron, 1992; Denneler *et al.*, 1999). The oldest living *F. nigra* specimens at Lake Duparquet have been dated to 1750–1770 (Tardif and Bergeron, 1999). *P. banksiana* is less long-lived (<100 year on average; Cayford and McRae, 1983; Rudolph and Laidly, 1990; Hofgaard *et al.*, 1999), and in

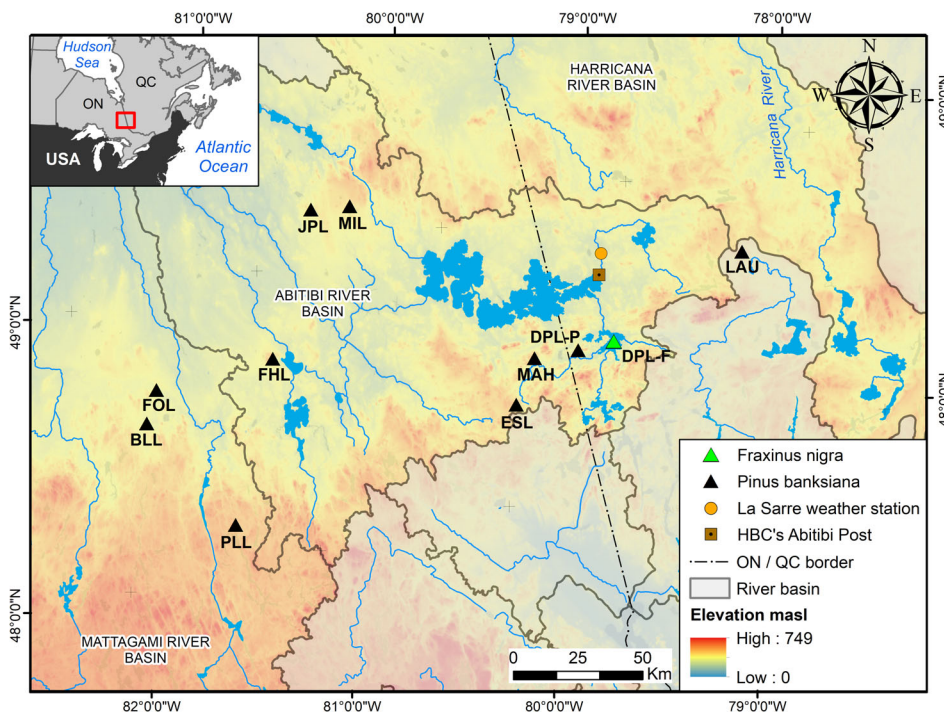


FIGURE 1 Map of the study area. *Pinus banksiana* (black triangles) and *Fraxinus nigra* (green triangle) sampling sites at the border between Ontario and Québec. River basin extents are provided for base map, and site codes are listed in Table 1 [Colour figure can be viewed at wileyonlinelibrary.com]

the absence of prolonged fire disturbance, the species is replaced by late successional ones (Cayford and McRae, 1983; Despons and Payette, 1992). *P. banksiana* chronologies can, however, be extended by using charred snags which are highly resistant to falling and decomposition compared to *Picea* and *Abies* spp. (Dansereau and Bergeron, 1993; Angers *et al.*, 2010). Standing dead trees charred during one or several fires can remain under the canopy for several hundred years and thus reflect the growing conditions of one or more generations of trees prior to fire (Dansereau and Bergeron, 1993; Angers *et al.*, 2010).

2.2 | Tree-ring data

During summer 2018, 722 samples were collected from 345 *P. banksiana* trees at 10 sites (Figure 1; Table 1) and including 45 samples (22 trees) from Dansereau and Bergeron (1993). Samples were prepared according to standard dendrochronological procedures (Cook and Kairiukstis, 1990) and crossdated using previous multi-century chronologies developed for *P. banksiana* (Bergeron and Dansereau, 1993; Hofgaard *et al.*, 1999; Girardin *et al.*, 2006). EW, LW, and total ring-width (RW) were measured using Coorecorder (v 9.6; Larsson, 2003a) and validated using both CDendro (v 9.6; Larsson, 2003b) and COFECHA (Holmes, 1983). Further dendrochronological details about the preparation of samples, pre-processing of chronologies to avoid biases from the influence of past fires on tree growth, as well as a climate-growth sensitivity analysis can be found in the Supporting Information Material S1.

Additionally, *F. nigra* anatomical and RW series developed in the floodplain of Lake Duparquet by Nolin *et al.* (2021b) were included in the tree-ring dataset and comprised an additional 62 series from 43 trees. *F. nigra* series were constituted of 12 variables including four RW variables (RW, EW, LW, and EW/RW proportion) and eight anatomical variables derived from the analysis of EW vessels (mean lumen cross-sectional area of the total, 25% largest, and 25% smallest vessels; total lumen cross-sectional area; number of vessels; porosity within the EW; density of vessels; and hydraulic conductivity diameter). Further details about these series are given in Nolin *et al.* (2021b).

2.3 | Climate data

Because few weather stations in our study area predate the 1950s (Girardin *et al.*, 2011) climate data were extracted from the KNMI Climate Explorer (<https://climexp.knmi.nl>; Trouet and Van Oldenborgh, 2013). Monthly mean gridded CRU TS4.04 (Harris *et al.*, 2020) temperature data were extracted from 1901 to 2019 and from a coordinate polygon corresponding to the spatial extent of the 11 sampling sites (48°N; -78°E-49°N; -81.5°E; Figure 1). From the same coordinate polygon, average land spring (March–May) temperatures from the Gridded Berkeley Earth Surface Temperature Anomaly Field (1750–2019; Rohde *et al.*, 2013) and the 20th Century Reanalysis V3 (1836–2015; Slivinski *et al.*, 2019) were downloaded as independent verification datasets for the reconstruction diagnostic. The Berkeley spring temperature is based on interpolation of an enhanced set of

TABLE 1 Tree-ring chronologies provenance

| Species | Site | Code | Latitude/ longitude | N trees | N series | Period | Average series length (years) |
|---------|----------------------|------|------------------------|---------|----------|-----------|----------------------------------|
| PIBA | Blue Lake | BLL | 48°34'N; 81°44'W | 19 | 39 | 1855–2017 | 105 |
| PIBA | Lake Duparquet | DPL | 48°28'N; 79°27'W | 45 | 91 | 1776–2017 | 108 |
| FRNI | Lake Duparquet | DPL | 48°28'N; 79°16'W | 43 | 62 | 1770–2016 | 64 |
| PIBA | Esler Lake | ESL | 48°20'N; 79°50'W | 35 | 76 | 1833–2017 | 75 |
| PIBA | Frederick House Lake | FHL | 48°41'N; 81°01'W | 40 | 80 | 1874–2017 | 103 |
| PIBA | Footprint Lake | FOL | 48°40'N; 81°39'W | 45 | 93 | 1746–2017 | 86 |
| PIBA | Jack Pine Lake | JPL | 49°10'N; 80°39'W | 29 | 65 | 1809–2017 | 90 |
| PIBA | Launay | LAU | 48°39'N; 78°30'W | 18 | 40 | 1867–2017 | 125 |
| PIBA | Magusi hills | MAH | 48°29'N; 79°41'W | 26 | 58 | 1777–2017 | 89 |
| PIBA | Mistango Lakes | MIL | 49°08'N; 80°26'W | 25 | 53 | 1766–2017 | 113 |
| PIBA | Peter Long Lake | PLL | 48°09'N; 81°24'W | 63 | 127 | 1723–2017 | 79 |

Note: Species are *Pinus banksiana* (PIBA) and *Fraxinus nigra* (FRNI). Code refers to Figure 1. (Period is the period after truncation to $n > 3$ samples to account for post-fire regeneration gaps in each site chronologies, cf. Supporting Information Material S1).

weather stations data and given as anomalies relative to January 1951–December 1980 (Rohde *et al.*, 2013). For the study area, the earliest climate observation of the Berkeley data corresponded to the spring of 1897 (Abitibi Post), and within a 500-km radius, the spring of 1866 (location [s] unknown). The Hudson's Bay Company fur trading post on Lake Abitibi (Abitibi Post, 48°43'N; 79°22'W; Figure 1) is the oldest local source of monthly temperatures with data recovered from 1897 to 1935 (years 1900, 1901, 1917, and 1922 missing; <https://climatedata.ca/>) and significantly correlating with Berkeley spring temperatures ($r = .96$, $p < .001$). Berkeley temperatures for the earlier period (1750–1866) are the results of interpolation of data from climate stations further away than 500 km (locations unknown; <http://berkeleyearth.lbl.gov/locations/49.03N-78.37W>). The 20th-Century Reanalysis, on the other hand, assimilates surface pressure observations and an ensemble of ocean–atmosphere circulation models to generate estimates of historical weather data (Slivinski *et al.*, 2019). This dataset provides a reliable historical context of surface temperature fields from synoptic to climatic time scale (Slivinski *et al.*, 2021).

To investigate the relationship between spring (March–May) temperature and regional to large-scale spring discharge, both instrumental (1915–2020; Water Survey of Canada, <https://wateroffice.ec.gc.ca>) and reconstructed Harricana River spring discharge (15 April–30 June; 1771–2016; Nolin *et al.*, 2021b), NOAA/NCDC Rutgers Snow Cover (March–May; 1967–2016; Estilow *et al.*, 2015), and monthly GRUN global gridded runoff (March–May; 1902–2014; Ghiggi *et al.*, 2019) were used. The reconstruction of the Harricana River spring discharge is derived from EW vessel cross-sectional area and ring width of *F. nigra* trees growing along the shores of Lake Duparquet, and periodically flooded in spring. The reconstruction captured 69% of the variance over a 102-year calibration period (1915–2016) and showed high coherency with regional flood-ring frequencies (Nolin *et al.*, 2021a) and various hydrological paleorecords from subarctic Québec (Nolin *et al.*, 2021b). Rutgers snow cover is a mapping of Northern Hemisphere snow extent, based on digitizing hand-drawn maps from shortwave satellite imagery (1967–1972; resolution ~ 4 km) and very high-resolution radiometer satellite imagery (after October 1972, resolution ~ 1 km; Estilow *et al.*, 2015). GRUN runoff is a multi-model ensemble of hydrological simulations trained with observational discharge data and climate data from a downscaled and corrected version of the 20th-Century Atmospheric Reanalysis and provided at a $5^\circ \times 5^\circ$ spatial scale (Ghiggi *et al.*, 2019). The association with Lake Duparquet spring ice break-up water level reconstructed from maximum ice-scar heights (Tardif and Bergeron, 1997) was also determined, as well as with

observational ice break-up dates (site DPL; Mongrain, 2014; Mongrain, personal communication 2018). To detect and characterize linear trends in observed hydrological and climatic time series, nonparametric Mann–Kendall trend statistic was used (Burn and Elnur, 2002; Monk *et al.*, 2011; Mortsch *et al.*, 2015).

2.4 | Reconstruction of temperatures

A composite temperature reconstruction was developed from nested principal component regression models (Cook *et al.*, 2003; Frank and Esper, 2005; Girardin *et al.*, 2006) to maximize both spatial and temporal coverage of the predictor chronologies constituted of 30 *P. banksiana* (10 sites \times 3 variables) and 12 *F. nigra* (1 site \times 12 variables) chronologies. This method involves splicing the total time span of the tree-ring data into sub-periods of common intervals to maximize the number of tree-ring predictors in sub-periods. Principal components analysis (PCA) was performed on each sub-period from a correlation matrix to transform the standard chronologies into a reduced number of linear combinations of the original chronologies with reduced multicollinearity (Meko and Graybill, 1995; Hidalgo *et al.*, 2000). Eigenvectors with an eigenvalue > 1 were retained as potential predictors following the Kaiser–Guttman rule in each model (Hidalgo *et al.*, 2000; Frank and Esper, 2005). Since tree growth can be influenced by temperature from the previous year, principal components lagged forward by 1 year ($t + 1$) were also included in the predictors set to reconstruct temperature for the current year (t) (Fritts, 1976; Briffa *et al.*, 1988).

Generalized additive mixed models (GAMMs; Wood, 2017) were used for the calibration of transfer function models needed for the spring temperature reconstruction. A GAMM is like a generalized linear mixed model, except that smooth terms are incorporated, which allows for a rich collection of the nonlinear relationships, including multiple forms of spline functions. First, a screening of PCA-reduced standard chronologies (t and $t + 1$) was done using stepwise multiple linear regression analysis (p -value to enter = .05; p -value to remove = .01). The model took the form:

$$T_{i,t} = \beta(i^{\text{th}}_{t,t+1}) + \varepsilon_{i,t} \quad (1)$$

where T is the spring temperature, i^{th} represents n^{th} principal components, t represents the year, and ε the residual error of each model. The preselected candidate predictors were then entered in a GAMM corresponding to each sub-period. Each GAMM model included nonlinear predictors (tree-ring data) to predict and

(temperature data) relationships. The GAMM equations took the form:

$$T_{i,t} = f(i^{\text{th}}_{t,t+1}) + \nu_i + \varepsilon_{i,t} \quad (2)$$

where ν_i is an error term with an AR1 ($p = 1, q = 0$) correlation structure. Smoothing function (f) of the GAMM were cubic regression splines with a degree of smoothness determined using a built-in cross-validation fitting process (Wood, 2003). The significance of predictors was re-evaluated within the GAMM models ($p < .10$) to avoid variance inflation in the final regression equations. The variables for which the smoothing terms were not significant in this first iteration were passed in a second GAMM iteration, this time in a linear form:

$$T_{i,j,t} = f(i^{\text{th}}_{t,t+1}) + \beta(j^{\text{th}}_{t,t+1}) + \nu_{ij} + \varepsilon_{i,j,t} \quad (3)$$

where j^{th} represents n^{th} principal components represented using a linear function (β). Predictors that did not satisfy the $p < .10$ requirement were removed. GAMM iterations were repeated until only significant predictors were included in the models. Fitted coefficients per periods (transfer functions) were then extracted from each GAMM model and applied to their respective PCs to get estimates of spring temperature over the period not covered by the instrumental data. Models' assumptions were validated using a standard analysis of the residuals, and each model was individually cross-calibrated and validated using the maximum period of overlap with instrumental data (116 years) split in half (1901–1958/1959–2016; 58 years). Final models were calibrated over the entire period of available temperature data (1901–2016). GAMM modelling was performed using the 'mgcv' package v.1.8–36 (Wood, 2021). Reconstruction efficiency and stability was assessed from the adjusted explained variance ($\text{Adj}R^2$) and Fisher's F statistic as well as from standard dendrochronological statistics reduction of error (RE, Briffa *et al.*, 1988) and coefficient of efficiency (CE, Cook and Kairiukstis, 1990), product-mean test (PMT), sign test, and mean absolute error (MAE, Cook *et al.*, 1999). All statistical procedures were conducted in R v.4.0.3 (R Core Team, 2021).

3 | RESULTS

3.1 | Reconstruction of spring temperatures

Twelve transfer functions were developed from the principal components of the tree-ring intra-annual width and

anatomical chronologies and constituted 12 regression models covering 12 sub-periods and spanning at most 1723–2016 and at least 1947–2016 (Figures 2a,b and S1; Table S1). Stepwise regressions selected the current year PC1 as the main predictor in each model. The first model (1954–2016) explained 54% of the variance in the observed data with five predictors selected. It also performed similarly in the split calibration-verification procedure (Table S1). Calibration R^2 and verification statistics of the following models decreased with the decline of the number of potential predictors (Figure 2c; Table S1). Positive RE and CE, and $\text{RE} > \text{CE}$ indicated that 9 of the 12 models covering the period 1770–2016 had predictive skill and that they could be merged in a composite reconstruction of mean spring temperature (Table S1). The four remaining models extending to the year 1723 were excluded from the following analyses (Table S1). The mean inter-correlation between the nine selected models also demonstrated a high consistency in the reconstructed regional temperature signal, with a mean Pearson $r = .83 \pm .08$ std (Figure S1). Overall, the reconstruction demonstrated good skill to track inter-annual variability and to reproduce the low-frequency patterns found in the instrumental spring temperature data with a slightly higher accuracy to capture mean negative (mean departure from instrumental data for negative values, $\bar{x} = -0.48 \pm 0.89$ std) than mean positive spring temperatures (mean departure from instrumental data for positive values, $\bar{x} = 0.95 \pm 0.77$ std) over the calibration period (1901–2016; Figure 2; Table S1). The accuracy of the reconstruction to capture extreme spring mean high and low temperatures, however, indicated a lower accuracy in capturing extreme low temperatures at the beginning of the century (1912, 1917, 1923, 1926, 1943, and 1950) and then a lower accuracy to capture extreme high temperatures at the end of the century (1977, 1986, 1987, and 2010; Figures 2 and S1). The average residuals for the 10 years of highest and lowest spring temperatures remained comparable between the two half-calibration periods but also evidenced the better reconstruction of lowest spring temperatures at the end of the century (1901–1958, average residuals for the 10 warmest springs 1.21 ± 0.85 std, and the coldest -1.38 ± 0.80 std; 1959–2016, average residuals for the 10 warmest springs 1.38 ± 0.83 std and the coldest -0.51 ± 0.83 std). The reconstructed mean spring temperature was significantly correlated with the Berkeley mean spring temperature record during the entire reconstructed period ($r = .49, p < .001, 1770-2015$; Figure 3c) and consistently across much of central-to-northeastern Canada (Figures 4a and 5a). Comparison with the mean spring temperature from the 20th-Century Reanalysis also indicated a consistent correlation with

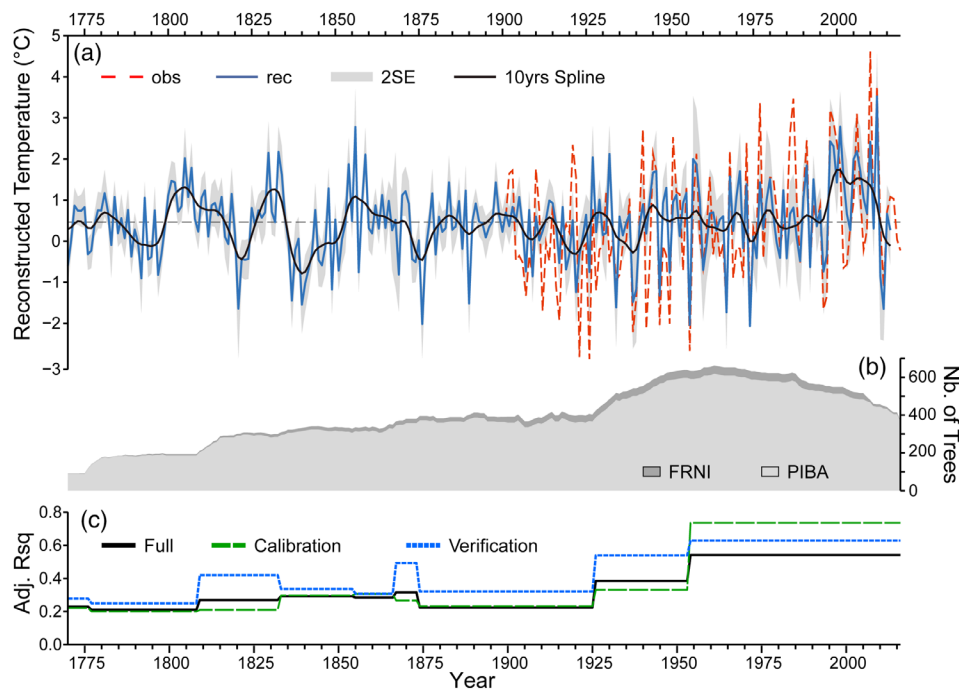


FIGURE 2 Characteristics of the composite temperature reconstruction. (a) Reconstruction of spring (March–May) temperature from 1770 to 2016 with two-standard-error confidence interval (grey) and decadal variation highlighted by a 10-year smoothing spline (black). Observed temperature data are illustrated by the dashed red line. A horizontal line delineates the reconstructed temperature mean at 0.41°C . (b) Sample depth of *Fraxinus nigra* (FRNI, dark grey) and *Pinus banksiana* (PIBA, light grey). (c) Adjusted multiple correlation coefficient (R^2) for each model periods and for the calibration (green), verification (blue), and full model (black) equations [Colour figure can be viewed at wileyonlinelibrary.com]

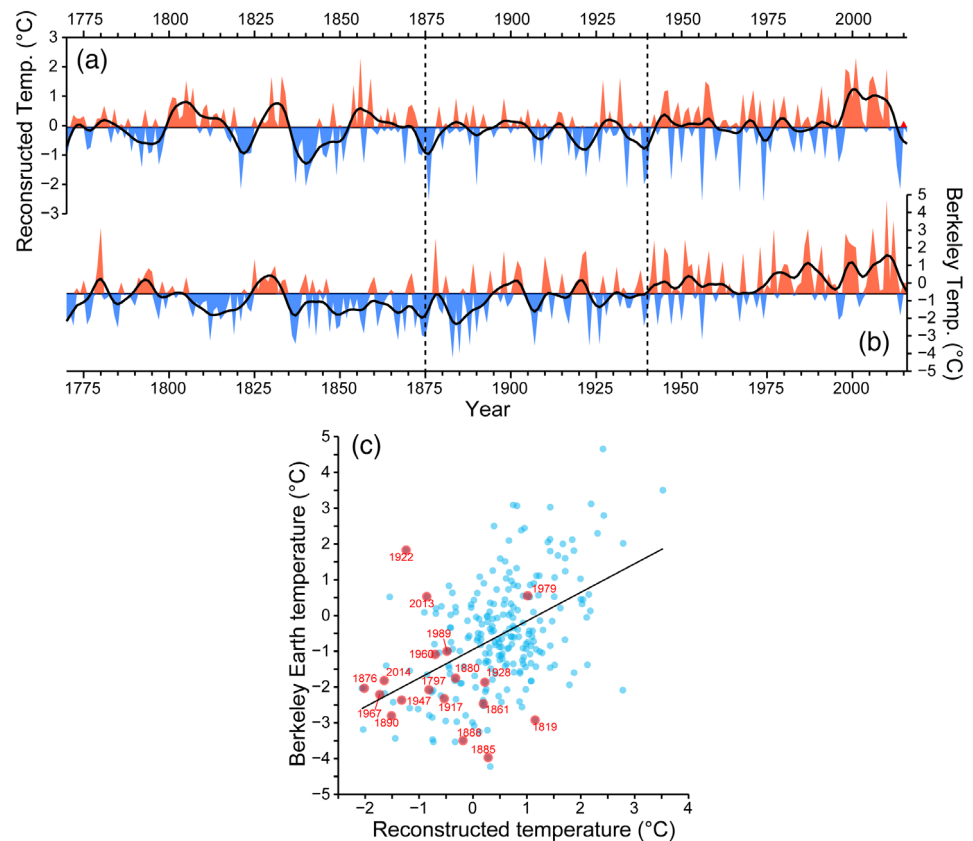
our spring temperature reconstruction ($r = .42$, $p < .001$, 1836–2015) and across a comparable spatial extent (Figure 5). To test the temporal and spatial stability of the associations between the reconstructed mean spring temperature over Canada, the Berkeley averaged spring temperature anomalies, and the spring mean temperature of the 20th-Century Reanalysis, 50-year Pearson correlation' windows lagged backward by 25 years were used (Figure 5). The results showed temporally consistent correlations centred on the study area, with the exception of the 1892–1941 interval where the spatial association decreased in the Great Lakes region in both datasets. The highest and most significant spatial correlations ($r > .60$; $p < .001$) with both datasets were found for the recent period and extending back to the beginning of the 19th century. The lower spatial correlation for the late 18th and early 19th centuries reflects the interpolation that has been done from climate stations located more than 500 km from the study area in the Berkeley record and revealing associations being significantly higher with northcentral USA than central Canada (Figure 5).

Three different periods can be distinguished in the reconstruction (Figures 2a and 3a). A first period lasting from 1770 to ~ 1875 was marked by persistent multidecadal cold and warm phases of comparable

amplitudes. This period lasted until the end of the Little Ice Age. From ~ 1875 to 1940, the amplitude in the decadal variability was reduced as highlighted by the 10-year smoothing spline (Figures 2a and 3a). After ~ 1940 , both the mean spring air temperature reconstruction and observational data were marked with a warm period contrasting with the last 250 years and a higher frequency of extreme warm spring temperatures. This third period (1940–2016) was also marked by the absence of multidecadal cold phase, and by the persistence of a warm phase lasting ~ 25 years (Figures 2a and 3a). The cold phase that lasted from the end of the Little Ice Age until the 1900s and the warming enhancement post the 1950s were more marked and persistent in the Berkeley record, albeit the two records (reconstruction and Berkeley) remained coherent at low frequency across those two periods (Figure 3).

Given that the mean monthly and seasonal CRU, and Berkeley temperature timeseries showed no AR (1) autocorrelation, Mann–Kendall linear trend investigation was conducted. Significant ($p < .05$) linear warming trend were indicated in the month of May and overall spring from 1901 to 2019 in observed CRU temperature ($\tau_{\text{MAR}} = 0.10$, $p = .110$; $\tau_{\text{APR}} = 0.10$, $p = .116$; $\tau_{\text{MAY}} = 0.17$, $p = .007$; and $\tau_{\text{SPRING}} = 0.17$, $p = .007$) and

FIGURE 3 Comparison from 1770 to 2016 between (a) reconstructed mean spring air temperature and (b) Berkeley mean spring air temperature. Warm and cold phases are illustrated respectively by red and blue areas and supported by a 10-year spline highlighting the decadal variability. Note that the two series are presented with a different y-axis range. Vertical dashed lines indicate the three periods (1770–1875, 1875–1940, 1940–2016) distinguished in the reconstruction. (c) Scatterplot of the two time-series showing the dispersion of their respective values (blue circles). Years highlighted by red circles indicate the ones with the highest discharge values in the reconstructed spring mean discharge of the Harricana River since 1770 (discharge higher than $151.3 \text{ m}^3 \cdot \text{s}^{-1}$; Nolin *et al.*, 2021a, 2021b) [Colour figure can be viewed at wileyonlinelibrary.com]



Berkeley records ($\tau_{\text{MAR}} = 0.13$, $p = .044$; $\tau_{\text{APR}} = 0.08$, $p = .175$; $\tau_{\text{MAY}} = 0.18$, $p = .005$; and $\tau_{\text{SPRING}} = 0.18$, $p = .004$). The Berkeley records also showed a significant warming trend in March, which was not detected in the CRU dataset. As for the mean spring temperature reconstruction, it showed a modest linear warming trend over a comparable period ($\tau = 0.14$, $p = .022$, 1901–2016).

Over the three periods (1770–1875, 1875–1940, 1940–2016) standard deviation in reconstructed mean spring temperature increased particularly since ~ 1940 in both positive (respectively, $\text{std} = 0.57, 0.47, 0.74$) and negative values (respectively, $\text{std} = 0.43, 0.57, 0.64$; Figures 2a and 3a). Compared to the Berkeley record, which only showed a steady increase in mean spring temperature, the calibration data and the reconstruction showed particularly low peaks of mean spring temperatures and especially after the 1930s (Figures 2a and 3). The last 40 years also showed less occurrence of extreme low spring temperature in each record (reconstruction, calibration data, Berkeley; Figures 2a and 3). For instance, over the period 1901–2019, observed spring mean temperature values below the mean minus 1.5SD threshold (-1.85°C) occurred in years 1917, 1923, 1926, 1939, 1943, 1947, 1950, and 1956, with the coldest temperature recorded being the spring of 1926 (-2.87°C). In comparison, during

the last 40 years (1980–2019) the coldest recorded temperature was -1.66°C in 1996.

3.2 | Relationship to spring flooding

The reconstructed spring mean temperature showed high coherency with spring paleoflood evidence from Lake Duparquet. The reconstruction was negatively and significantly correlated with the Harricana River spring (15 April–30 June) mean discharge in both reconstructed ($r = -.52$; $p < .001$; 1771–2016) and instrumental ($r = -.55$; $p < .001$; 1915–2016) dataset. Correlations with instrumental monthly mean and maximum discharge of the Harricana River (1915–2016) also showed that the reconstructed mean spring temperature was more strongly associated to late spring stage ($r_{\text{mean MAY}} = -.61$; $r_{\text{max MAY}} = -.54$; $r_{\text{mean JUN}} = -.58$; $r_{\text{max JUN}} = -.62$; all $p < .001$) than to early spring stage of the river ($r_{\text{mean MAR}} = .23$; $p = .019$; $r_{\text{max MAR}} = .29$; $p = .003$; $r_{\text{mean APR}} = .33$; $p = .001$; $r_{\text{max APR}} = .11$; $p = .271$). Correlations with averaged spring discharge (March–May) further demonstrated that the reconstructed mean spring temperature was more strongly associated to the spring maximum ($r = -.50$; $p < .001$) than to spring

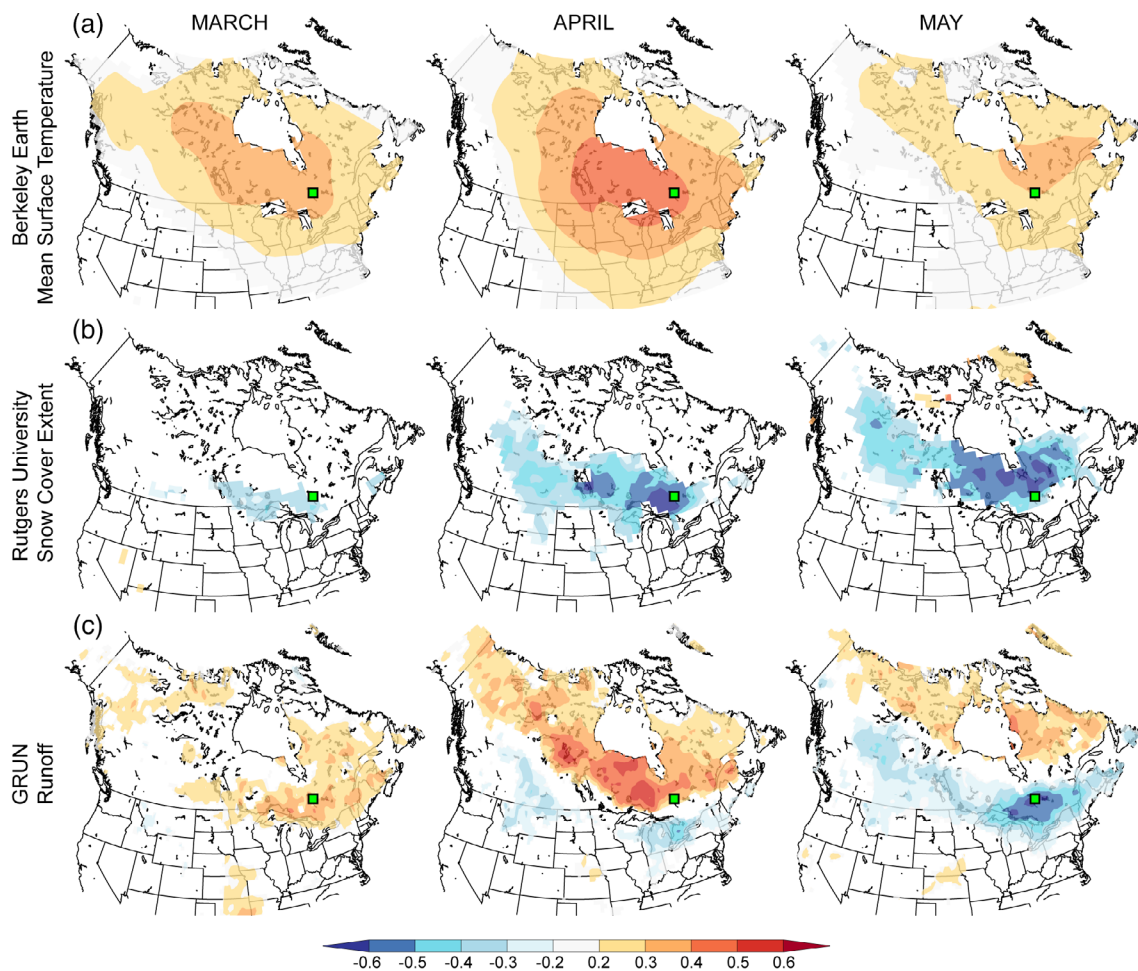


FIGURE 4 Spatial correlation maps ($p < .10$) between reconstructed spring mean air temperature and March–May. (a) Berkeley average temperature anomalies (1770–2016); (b) NOAA Rutgers snow cover (1967–2016); and (c) GRUN runoff (1902–2014). Correlation coefficients range from positive (red) to negative (blue). Spatial correlations were done using the KNMI Climate Explorer engine (<https://climexp.knmi.nl>; Trouet and Van Oldenborgh, 2013). Green square symbol indicates the study area [Colour figure can be viewed at wileyonlinelibrary.com]

mean discharge ($r = -.22$; $p = .030$). In the Harricana River, maximum discharge occurred on average on 8 May and ranged between 14 April and 29 May (1915–2020). The mean spring temperature reconstruction was also negatively and significantly correlated with observed ice break-up date ($r = -.54$; $p < .001$; 1968–2016) and spring lake water levels reconstructed from a maximum ice-scar height chronology ($r = -.25$; $p < .001$; 1770–1990) for Lake Duparquet. The ice break-up at Lake Duparquet over the period 1968–2016 occurred on average on 9 May and ranged between 20 April and 24 May. No significant linear trend towards earlier ice break-up was found in annual ice break-up dates for Lake Duparquet (Mann–Kendall $\tau = -.014$; $p = .162$; 1968–2018).

In the spring temperature reconstruction, most years with the lowest mean spring temperature calculated per decade (1771–1779, 1780–1789, ..., 2000–2009, 2010–2016;

Table 2) corresponded to the most severe spring flood years reconstructed for the last 250 years (1771–2016). A total of 14 years of minimum spring temperature (1797, 1861, 1876, 1880, 1888, 1890, 1917, 1922, 1947, 1960, 1967, 1989, 2013, 2014, and 2019 also but outside of the calibration period) matched 14 of the 18 years of highest spring discharge reconstructed since 1771 (the 1819, 1885, 1928, and 1979 floods did not match; Table 2). Similar results were obtained using the instrumental Harricana River spring discharge over the 1920–2016 period (1922, 1947, 1960, 1967, 1989, 2013, 2019 also but outside the calibration period), at the exception of year 2014 ($127.21 \text{ m}^3 \cdot \text{s}^{-1}$; Table 2). While most of the minimum mean temperatures per decade were below zero, no apparent threshold at which the temperature corresponds to a high spring flood discharge was discernible (Table 2). The coldest reconstructed spring years also did not always correspond to the highest spring discharge (Table 2).

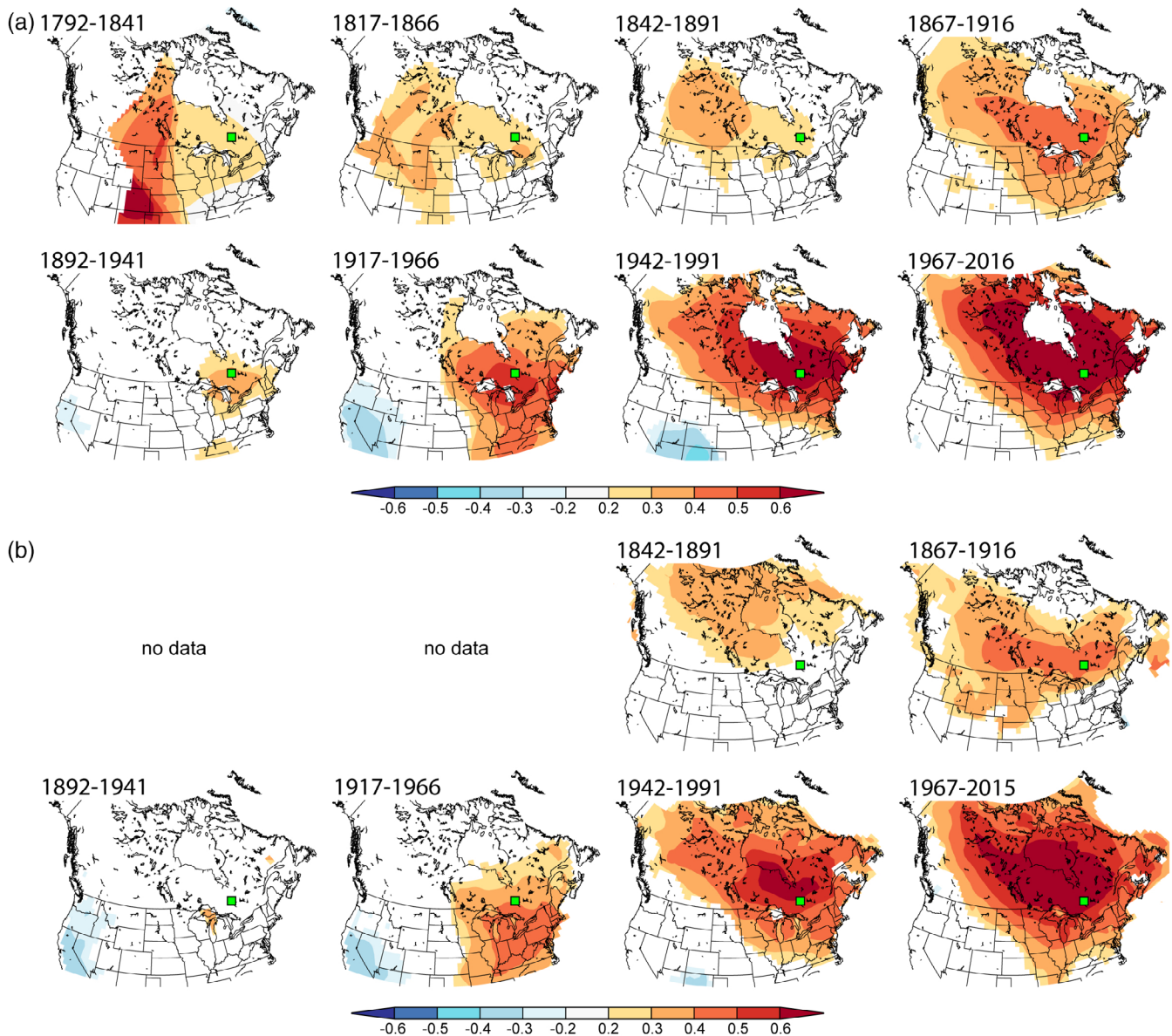


FIGURE 5 Spatial correlation maps ($p < .10$) between reconstructed mean spring air temperature and (a) Berkeley spring average temperature anomalies, and (b) 20th-Century Reanalysis average spring temperature. Correlations are given for 50-year moving windows lagged backward by 25 years and were done using the KNMI Climate Explorer Engine (<https://climexp.knmi.nl>; Trouet and Van Oldenborgh, 2013). Green square symbol indicates the study area [Colour figure can be viewed at wileyonlinelibrary.com]

Significant and negative association was found between the reconstructed mean spring temperature and the last day with snow on the ground over the study area, calculated from daily Rutgers Snow Cover values as the first day with a value < 0.1 in spring ($r = -.42$, $p < .001$; 1967–2016). Investigating spatial field correlations indicated strong and negative associations between reconstructed spring mean temperature and spring snow cover extent across much of central to northeastern boreal Canada (Figure 4b). Associations were strongest in late spring (April, May) and

particularly in May with the highest correlations found over the study area and extending to the James Bay and the Great Lakes (Figure 4b). Used for validation purposes, spatial correlations of the reconstructed mean spring temperature with GRUN runoff indicated positive associations in March–April across much of northern Canada switching to negative associations in May over our study area (Figure 4c), which is in line with the change in the sign of correlation found in the correlation with instrumental Harricana River mean and maximum discharge.

TABLE 2 Comparison of reconstructed mean spring (March–May) temperature minimums and of reconstructed and instrumental mean spring (15 April–30 June) discharge maximums

| Decade | REC temperature | | REC discharge | | HAR discharge | |
|-----------|---------------------|---------------------|----------------------|----------------------|----------------------|----------------------|
| | First min | Second min | First max | Second max | First max | Second max |
| 1771–1779 | 1770 (–0.60) | 1776 (–0.32) | 1771 (121.75) | 1773 (118.24) | / | / |
| 1780–1789 | 1789 (–0.38) | 1783 (–0.09) | 1789 (147.36) | 1787 (146.60) | / | / |
| 1790–1799 | 1792 (–0.90) | 1797 (–0.82) | 1797 (161.00) | 1792 (143.92) | / | / |
| 1800–1809 | 1809 (0.23) | 1808 (0.54) | 1808 (139.16) | 1802 (122.11) | / | / |
| 1810–1819 | 1818 (–0.07) | 1816 (0.11) | 1819 (157.43) | 1818 (148.66) | / | / |
| 1820–1829 | 1821 (–1.64) | 1823 (–0.45) | 1822 (150.29) | 1826 (148.88) | / | / |
| 1830–1839 | 1837 (–1.44) | 1838 (–0.21) | 1937 (145.53) | 1838 (125.09) | / | / |
| 1840–1849 | 1840 (–1.55) | 1849 (–1.18) | 1840 (150.69) | 1845 (135.12) | / | / |
| 1850–1859 | 1857 (–0.76) | 1851 (–0.72) | 1857 (146.67) | 1853 (132.10) | / | / |
| 1860–1869 | 1869 (–0.81) | 1861 (0.19) | 1861 (153.64) | 1867 (132.11) | / | / |
| 1870–1879 | 1876 (–2.02) | 1874 (–0.51) | 1876 (171.29) | 1873 (147.39) | / | / |
| 1880–1889 | 1880 (–0.32) | 1888 (–0.19) | 1888 (164.57) | 1880 (160.10) | / | / |
| 1890–1899 | 1890 (–1.51) | 1895 (0.09) | 1890 (170.25) | 1899 (133.51) | / | / |
| 1900–1909 | 1909 (–0.85) | 1907 (–0.74) | 1907 (151.05) | 1909 (149.43) | / | / |
| 1910–1919 | 1919 (–0.69) | 1917 (–0.53) | 1917 (159.52) | 1919 (140.75) | / | / |
| 1920–1929 | 1922 (–1.24) | 1926 (–0.75) | 1928 (175.57) | 1922 (173.66) | 1928 (191.15) | 1922 (165.27) |
| 1930–1939 | 1934 (–1.61) | 1939 (–1.48) | 1939 (137.34) | 1930 (132.86) | 1933 (160.68) | 1939 (151.64) |
| 1940–1949 | 1947 (–1.32) | 1940 (–1.17) | 1947 (177.34) | 1949 (133.73) | 1947 (189.79) | 1949 (143.99) |
| 1950–1959 | 1956 (–2.04) | 1950 (–0.77) | 1950 (134.24) | 1956 (125.02) | 1952 (128.15) | 1956 (128.02) |
| 1960–1969 | 1967 (–1.73) | 1960 (–0.7) | 1960 (179.95) | 1967 (163.59) | 1960 (196.10) | 1967 (171.12) |
| 1970–1979 | 1974 (–2.06) | 1976 (–0.41) | 1979 (184.86) | 1974 (147.05) | 1974 (179.85) | 1979 (167.19) |
| 1980–1989 | 1989 (–0.48) | 1985 (–0.42) | 1989 (161.72) | 1983 (144.61) | 1986 (152.84) | 1989 (149.16) |
| 1990–1999 | 1996 (–0.74) | 1992 (–0.63) | 1996 (144.31) | 1995 (125.07) | 1997 (131.21) | 1990 (125.91) |
| 2000–2009 | 2004 (0.27) | 2003 (0.66) | 2009 (138.62) | 2008 (133.51) | 2004 (141.97) | 2009 (141.58) |
| 2010–2016 | 2014 (–1.65) | 2013 (–0.86) | 2013 (170.90) | 2014 (160.52) | 2013 (156.90) | 2017 (152.35) |

Note: Values are compared by decade and for the last 247 years. ‘REC discharge’ is the reconstructed mean spring discharge of the Harricana River (1771–2016) and is taken from Nolin *et al.* (2021b). ‘HAR discharge’ is the instrumental mean Harricana River spring discharge (1915–2020). Both mean spring discharges are average from 15 April to 30 June daily discharge data, while temperature reconstruction is average March–May. Years in bold highlight the years that has been part of the highest mean spring discharge years since 1771. Grey cells highlight the years for which, per decade, the minimum spring temperature corresponds to the maximum spring discharge. The first (1771–1779) and last (2010–2016) periods used for comparisons are not complete decades.

4 | DISCUSSION

The reconstructed spring mean air temperature demonstrated evidence of a warming phase over the last century compared to the successive warm and cold persistent decadal phases observed up to the end of the Little Ice Age (1850–1870 CE). The coldest interval reconstructed that is, for the period ~1815–1855, is in line with tree-ring reconstruction of summer temperature published in sub-arctic Québec (Jacoby *et al.*, 1988; Briffa *et al.*, 1994; Gennaretti *et al.*, 2014; 2017) depicting this period as the coldest in the last millennium. The ~1815–1865 cold phases in northern Québec coincide with low solar

activity (Guiot, 1987) and active volcanic decades (notably the April 1815 eruption of Mount Tambora, Indonesia; Jacoby *et al.*, 1988; Briffa *et al.*, 1994; Gennaretti *et al.*, 2014; 2017). Both the observed CRU temperature and Berkeley records demonstrated significant warming of May and overall, of spring over the 1901–2019 period and the greatest reconstructed warming in spring mean air temperature has been detected starting since about 1940.

Observed maximum discharge of the Harricana River (1915–2020) and ice break-up dates for Lake Duparquet (1968–2018) also indicated that the onset of spring flooding over the 20th century occurred on average in

late April and early May. This suggests that air temperature in March and April may have had a greater influence on flood initiation than air temperature in May. While across Canada, minimum, mean, and maximum spring temperatures have generally warmed since 1950 (Zhang *et al.*, 2001a), the projected mid-century (2030–2059) monthly temperature changes of the Great Lakes Basin also suggest that future increases in maximum temperatures are likely to be higher from May to October than in any other months, and with the smallest increase found in April (Zhang *et al.*, 2018). The influence of the warming phase of spring temperatures reconstructed since ~1940 must therefore be put into perspective when analysing the relationship between spring temperature and flooding since significant linear warming trend in observed data was mostly found in May.

Independent regional studies already identified the 1850–1870s and 1930–1950s as breakpoints in the regional hydroclimate history. For instance, ice-scar frequencies and lake level changes for Lake Duparquet (Tardif and Bergeron, 1997) and other lakes from high-boreal Québec (Lemay and Begin, 2008; Boucher *et al.*, 2011) pointed towards an increase in the magnitude and frequency of flooding since the end of the Little Ice Age and increasing since the 1930–1950s. Reconstruction of spring discharge in the Harricana River associated recent increases in flood frequency and magnitude with cold, snowy winters, and late springs. Late spring snowmelt under the combined effect of spring precipitation and cold spring temperature marked the highest discharges of the century (Nolin *et al.*, 2021b). High spatial coherency was found in this study between spring mean air temperature, the snow cover extent, and the GRUN runoff. This result demonstrates the consistent control of spring temperature over snowmelt and runoff over central to northeastern Canada and particularly in late spring. The change in the sign of correlation between temperature, instrumental Harricana River discharge, and GRUN runoff suggests that discharge in March and April was associated to warm and early springs (positive correlation), and that discharge in May (and June) was associated to cold and late springs (negative correlation) with a persistent and thick snowpack. However, no significant linear trend was found in annual ice break-up dates for Lake Duparquet to support a trend towards earlier spring flooding. Indeed, per decade, much of the late and cold spring years were associated with the highest spring discharge years reconstructed for the Harricana River over the last 250 years (except for the years 1819, 1885), which was also supported by instrumental discharge data (except for year 2014). The years 1819 and 1885 represent regional contrasts in spring flooding with moderate flood-ring relative frequencies recorded in regional rivers

contrasting with high flood-ring frequencies and EW vessel records in Harricana River and Lake Duparquet (Nolin *et al.*, 2021a; 2021b).

It should be noted that the *F. nigra* series from Lake Duparquet (43 trees) were used to reconstruct the mean spring discharge of the Harricana River. The present reconstruction of mean spring temperature contains these same 43 series (11% of the trees used), reduced in PC components with 345 other *P. banksiana* tree series (Table 1). The detrending of *F. nigra* series was also not the same in both studies (smoothing spline with a 50% frequency of response at 60 years in Nolin *et al.*, 2021b; generalized negative exponential model detrending in this study; cf. Supporting Information Material S1). The use of the same proxies (43 trees) in both the Harricana River mean spring discharge and regional mean spring temperature reconstructions may influence the correlation between the two reconstructions. The decadal comparison between mean spring temperature and Harricana River mean spring discharge (1920–2016; Table 2), however, showed that results between instrumental and reconstructed Harricana River mean spring discharge were similar.

The variance explained by the present reconstruction (23–54%) is somewhat in the range of summer temperature reconstructions conducted over northeastern Canada using total RW of coniferous trees (Jacoby *et al.*, 1988; Gennaretti *et al.*, 2014) or multiproxy tree-ring approaches (Jacoby *et al.*, 1988; Briffa *et al.*, 1994). The present reconstruction underestimates extreme cold spring temperatures at the beginning of the century, and extreme high temperatures at the end of the century. Possible reasons include (a) the difficulty to capture a spring climate signal at the beginning of the growing season using dendrochronological proxies (Schweingruber, 1996; Rossi *et al.*, 2013); (b) the spatial and temporal heterogeneity of historical data in the early calibration period (Girardin *et al.*, 2011); (c) the diminution of tree-ring predictors going back in time; and (d) spring temperature variability and extremes that are not captured by tree ring proxies as tree-growth is never 100% explained by climate factors (McCarroll *et al.*, 2015). Indeed, the initiation of the tree-ring growth remain difficult to defined climatically (Schweingruber, 1996; Rossi *et al.*, 2013) and some of the variance in early spring temperatures might not be fully captured by *P. banksiana* trees if warm temperatures arise when trees have not yet begun their cambial activity. For example, in this reconstruction, the springs 1987 and 2010 showed the largest underestimation of extreme high spring temperature observed during the calibration period. The years 1987 and 2010 are among the three earliest breakups recorded at Lake Duparquet since 1968, along with the year 1998 (1987: 23 April; 1998: 23 April; and 2010: 22 April; 1968–2018 average being 9 May).

Observed CRU mean April temperature since 1901 were also highest in years 1955, 1984, 1987, and 2010 with values ranging from 4.84 to 5.25°C, as compared to a mean April temperature of 0.77°C over the 1901–2019 period.

Increases in the magnitude of both extreme warm and extreme cold reconstructed spring mean temperatures during the 1930s–1970s contrast with those reconstructed over the 1770–2016 period. These extremes also contrast with the Berkeley record but are consistent with our calibration data set. During the early stages of global warming (1930s), it is likely that the increase in near-freezing temperatures instead of below-freezing temperatures in winter and spring favoured precipitation (snow and/or rain) and quicker melting (Davis *et al.*, 1999; Zhang *et al.*, 2000; 2001b). One hypothesis could be that the occurrence of both cold (late spring, long-lasting snow cover) and warm extremes (early spring, quicker snowmelt) increased the frequency and magnitude of flooding observed in the region since 1930–1950 (Tardif and Bergeron, 1997; Nolin *et al.*, 2021a; 2021b) although this hypothesis still requires to be confirmed. Tardif and Bergeron (1997) had hypothesized that earlier spring melt with heavy rainfall could increase the risk of ice-breakup at a time the ice cover is thick, thus increasing the magnitude of flooding. The reduction in the number of cold springs in the last 40 years of the reconstructed and observed spring mean temperature would also contrast with the assumption that spring floods are for the most part due to snowmelt during cold and late springs. This result indicates that warmer late spring mean temperatures on average may contribute, among other factors, to advance the spring break-up and to likely shift the contribution of snow to rain in spring flooding processes. Such change in flooding processes have already been reported in Canada since about the 1950s (Burn and Whitfield, 2016; Aygün *et al.*, 2019; Bush and Lemmen, 2019) and similar trends are projected by most hydrological simulations across Canada and for Québec (Guay *et al.*, 2015; Gaur *et al.*, 2018; Bush and Lemmen, 2019). Warmer winter temperatures in northern Canada are expected to reduce snow accumulation and promote mid-winter melt, which should contribute to a decrease in SWE, while warmer spring temperatures are expected to accelerate snowmelt (Aygün *et al.*, 2019; Bush and Lemmen, 2019). Warmer spring temperature in northern Canada should also increase the likelihood of rain-on-snow events as well as the spring rainfall to snowfall ratio in future years (Zhang *et al.*, 2000; Ashmore and Church, 2001; Bush and Lemmen, 2019). Snow water equivalent had however increased in northern and central Québec since 1950 (Brown, 2010; Aygün *et al.*, 2019). In terms of timing, earlier freeze-up and break-up trends have been observed in south-central

Ontario since the 1900s (Fu and Yao, 2015), but not at Lake Duparquet. Using a cluster analysis of the Harricana River daily hydrographs, Nolin *et al.* (2021b) also noted that early spring break-ups with minimal to intermediate discharge dominated between 1998 and 2012 when compared to the period 1914–2020. Our present results further showed an inverse relationship between the reconstructed mean spring temperature and the last day with snow on the ground over our study area and for the 1967–2016 period.

Climate model simulations for the whole Québec project a +10% to +15% increase in precipitation (from south to north) by 2050 with a net change in winter and spring precipitation forms, contributing to a 0–5% increase (again from south to north) in the contribution of winter months to annual streamflow, and an increase in average spring flood volume of about 5% (Guay *et al.*, 2015). The frequency of extremes and their maximum magnitudes are also expected to increase by up to +20% for Québec by 2070 led by rain instead of snow (Clavet-Gaumont *et al.*, 2017). At this point, it remains hazardous to clearly dissociate a snowmelt-driven flood from a rainfall-driven flood in our study area, and it remains to be determined how the increase in spring temperatures, the reduction in snow cover, and the increase in rainfall will interact with the flood regime in snowmelt driven river basins. For instance, the years 1989 and 1999 in the Harricana River were characterized by two peaks triggered by the snowmelt in late spring, and by heavy precipitation event in early summer (not shown).

Future research could aim at a reconstruction of precipitation or of snow parameters (e.g., snow cover extent, snow depth, or snow water equivalent) to further investigate the relationship between precipitation, snowmelt, and flooding and allow to predict consistent hydroclimatic trajectories under various climate change scenarios. For instance, Mood *et al.* (2020) developed a reconstruction of the snowpack variability from annual RWs of high-elevation Pacific Silver Fir (*Abies amabilis* Douglas ex. J. Forbes) in British Columbia. Similar reconstructions also come from areas where tree growth is more water limited. For instance, Touchan *et al.* (2021) reconstructed multi-millennial variability on 1st April SWE from EW and LW width chronologies of Giant Sequoia (*Sequoiadendron giganteum* J. Buchh. ex Lindl.) in California and Colorado, USA. The studies of Mood *et al.*, 2020 and Touchan *et al.*, 2021 benefited from manual snow records since the 1950s to calibrate the tree-ring predictors. In the same way, Shamir *et al.* (2020) used principal components analysis of snowpack-related climatic variables, derived from a high-resolution hydrological model, to explain respectively 48 and 35% of the variance in EW and latewood width chronologies of four

coniferous tree species growing in mountains of central Sierra Nevada, USA. Overall, these results suggest that tree species responding to climate parameters of the early growing season, such as *P. banksiana* and *F. nigra* might be suitable candidates to reconstruct snow variability and further investigate the relationships between spring snow cover, temperature and flooding.

5 | CONCLUSION

This study presents a new *P. banksiana* tree-ring network and a well-verified reconstruction of regional spring mean air temperature consistent across much of central-to-northeastern Canada and since year 1770. The 12 transfer functions calculated explained 23–54% of the observed spring mean temperature variability over the last 247 years with a decreasing efficiency back in time which correspond mainly to the decrease in the number of available tree-ring data in the early years of the reconstruction. The end of the Little Ice Age was characterized by cooler than average springs and multidecadal cold and warm phases before transitioning towards a warming of late spring (May) temperature, and particularly after the 1940s and in the last 40 years. Most of the highest spring flooding reconstructed in the nearby Harricana River matched with the decadal variability reconstructed in low spring temperature. The coherency found with the snow cover extent and the gridded runoff across much of central-to-northeastern Canada also support that high historical spring flooding were mainly triggered by long lasting snow cover in late spring. However, over the last 40 years of the reconstruction, the reduction in the number of cold springs may suggest that spring flooding may now be related less to the persistence of late spring snow cover, but rather to earlier snowmelt and increased precipitation contribution to discharge. These changes in boreal hydrology and flooding appear to be a likely consequence of the recent warming trend observed in mean spring temperatures. Further research is needed to understand whether changes have occurred in the distinct contributions of current snow and precipitation to spring flooding to allow for reliable regional hydroclimatic trajectory projections. Among other things, it will be necessary to determine whether or not future changes in spring temperature will lead to changes in the relative supply of rain and snow to the spring flood dynamics in eastern boreal Canada.

ACKNOWLEDGEMENTS

The authors would like to thank the field and laboratory assistants Marion Cartier, Cyrielle Ducrot, Ralitsa Mincheva, and especially Isabelle Gareau for their thorough work. They also acknowledge the special support of

the Forêt d'Enseignement et de Recherche du Lac Duparquet (FERLD) research station team for their support during the field campaigns and laboratory procedures and especially Danielle Charron and Raynald Julien. Locating old growth *Pinus banksiana* stands in northern Ontario was made possible with special support from Lars Hildebrandt and Bonny Fournier (Ontario Forest Service). This study was a contribution of Canada Research Chairs (NSERC-CRC) hold by Yves Bergeron and Jacques Clément Tardif and was funded by the Natural Sciences and Engineering Research Council of Canada Collaborative Research program including our partners Ouranos, Hydro-Québec, Ontario Power Generation (OPG), and The University of Winnipeg. This work was also supported by a scholarship from RIISQ – Intersectorial Flood Network of Québec (2nd program 2020–2021) awarded to Alexandre Florent Nolin. Earlier versions of the manuscript benefited from constructive comments by Susanne Kames (University of Winnipeg), David Huard (Ouranos), and Kurt Kornelsen (OPG). They would also like to thank the contributions of the Associate Editor Dr Jose Marengo and two anonymous reviewers who provided constructive comments and suggestions on earlier drafts of the manuscript.

AUTHOR CONTRIBUTIONS

Alexandre Florent Nolin: Conceptualization; formal analysis; investigation; methodology; visualization; writing – original draft; writing – review and editing. **Martin Philippe Girardin:** Conceptualization; formal analysis; investigation; methodology; resources; validation; writing – review and editing. **Jacques Clément Tardif:** Conceptualization; formal analysis; funding acquisition; investigation; methodology; project administration; resources; supervision; validation; writing – review and editing. **Xiao Jing Guo:** Formal analysis; investigation; resources; software. **France Conciatori:** Data curation; investigation; methodology; resources; writing – review and editing. **Yves Bergeron:** Conceptualization; funding acquisition; project administration; resources; supervision; validation; writing – review and editing.

CONFLICT OF INTERESTS

The authors declare no potential conflict of interest.

DATA AVAILABILITY STATEMENT

Relevant data for this study are available from Nolin, A. F., Girardin, M. P., Tardif, J. C., Guo, X. J., Conciatori, F., & Bergeron, Y. (2021) *Pinus banksiana* and *Fraxinus nigra* dataset for the study of spring temperature in eastern boreal Canada. Mendeley Data, v1. <https://doi.org/10.17632/kk2rsk7rj6.1>. Data include tree-ring width and wood anatomical chronologies (PIBA_FRNI_Chronos.csv)

with their respective sample depth (PIBA_FRNI_SampDepth.csv) and the reconstructed spring mean temperature (PIBA_FRNI_RecSpringTemp.csv), as well as the GPS position of the sampling sites (LAT_LON_RecSpringTemp.kml), and a set of self-explanatory instructions and descriptions for data files (metadata.txt). All other data are available upon request to the corresponding author at alexandreflorent.nolin@uqat.ca (institutional email), alexandreflorent.nolin@gmail.com (permanent email).

ORCID

Alexandre Florent Nolin  <https://orcid.org/0000-0003-1033-9123>

REFERENCES

- Anchukaitis, K.J., D'Arrigo, R.D., Andreu-Hayles, L., Frank, D., Verstege, A., Curtis, A., Buckley, B.M., Jacoby, G.C. and Cook, E.R. (2013) Tree-ring-reconstructed summer temperatures from northwestern North America during the last nine centuries. *Journal of Climate*, 26(10), 3001–3012. <https://doi.org/10.1175/JCLI-D-11-00139.1>.
- Angers, V.A., Drapeau, P. and Bergeron, Y. (2010) Snag degradation pathways of four North American boreal tree species. *Forest Ecology and Management*, 259(3), 246–256. <https://doi.org/10.1016/j.foreco.2009.09.026>.
- Ashmore, P., & Church, M. (2001). The impact of climate change on rivers and river processes in Canada. Geological Survey of Canada, Bulletin 555. <https://doi.org/10.4095/211891>
- Aygün, O., Kinnard, C. and Campeau, S. (2019) Impacts of climate change on the hydrology of northern midlatitude cold regions. *Progress in Physical Geography: Earth and Environment*, 44(3), 338–375. <https://doi.org/10.1177/0309133319878123>.
- Ballesteros-Cánovas, J.A., Bombino, G., D'Agostino, D., Denisi, P., Labate, A., Stoffel, M., Demetrio, A.Z. and Zimbone, S.M. (2020) Tree-ring based, regional-scale reconstruction of flash floods in Mediterranean mountain torrents. *Catena*, 189, 104481. <https://doi.org/10.1016/j.catena.2020.104481>.
- Barber, V.A., Juday, G.P., Finney, B.P. and Wilmking, M. (2004) Reconstruction of summer temperatures in interior Alaska from tree-ring proxies: evidence for changing synoptic climate regimes. *Climatic Change*, 63(1), 91–120. <https://doi.org/10.1023/B:CLIM.0000018501.98266.55>.
- Bergeron, Y. (2000) Species and stand dynamics in the mixed woods of Quebec's southern boreal forest. *Ecology*, 81(6), 1500–1516. [https://doi.org/10.1890/0012-9658\(2000\)081\[1500:SASDIT\]2.0.CO;2](https://doi.org/10.1890/0012-9658(2000)081[1500:SASDIT]2.0.CO;2).
- Bergeron, Y. and Dansereau, P.R. (1993) Predicting the composition of Canadian southern boreal forest in different fire cycles. *Journal of Vegetation Science*, 4(6), 827–832. <https://doi.org/10.2307/3235621>.
- Boucher, É., Ouarda, T.B., Bégin, Y. and Nicault, A. (2011) Spring flood reconstruction from continuous and discrete tree ring series. *Water Resources Research*, 47(7), W07516. <https://doi.org/10.1029/2010WR010131>.
- Briffa, K.R., Jones, P.D., Pilcher, J.R. and Hughes, M.K. (1988) Reconstructing summer temperatures in northern Fennoscandia back to AD 1700 using tree-ring data from scots pine. *Arctic and Alpine Research*, 20(4), 385–394. <https://doi.org/10.1080/00040851.1988.12002691>.
- Briffa, K.R., Jones, P.D. and Schweingruber, F.H. (1994) Summer temperatures across northern North America: regional reconstructions from 1760 using tree-ring densities. *Journal of Geophysical Research: Atmospheres*, 99(D12), 25835–25844. <https://doi.org/10.1029/94JD02007>.
- Briffa, K.R., Osborn, T.J., Schweingruber, F.H., Harris, I.C., Jones, P.D., Shiyatov, S.G. and Vaganov, E.A. (2001) Low-frequency temperature variations from a northern tree ring density network. *Journal of Geophysical Research: Atmospheres*, 106(D3), 2929–2941. <https://doi.org/10.1029/2000JD900617>.
- Brown, R.D. (2010) Analysis of snow cover variability and change in Québec, 1948–2005. *Hydrological Processes*, 24(14), 1929–1954. <https://doi.org/10.1002/hyp.7565>.
- Burn, D.H. and Elnur, M.A.H. (2002) Detection of hydrologic trends and variability. *Journal of Hydrology*, 255(1–4), 107–122. [https://doi.org/10.1016/S0022-1694\(01\)00514-5](https://doi.org/10.1016/S0022-1694(01)00514-5).
- Burn, D.H. and Whitfield, P.H. (2016) Changes in floods and flood regimes in Canada. *Canadian Water Resources Journal*, 41(1–2), 139–150. <https://doi.org/10.1080/07011784.2015.1026844>.
- Burn, D.H. and Whitfield, P.H. (2017) Changes in cold region flood regimes inferred from long-record reference gauging stations. *Water Resources Research*, 53(4), 2643–2658. <https://doi.org/10.1002/2016WR020108>.
- Bush, E., Lemmen, D.S. (2019). Canada's Changing Climate Report. Government of Canada, Ottawa, ON, Canada. (p. 444).
- Buttle, J.M., Allen, D.M., Caissie, D., Davison, B., Hayashi, M., Peters, D.L., Pomeroy, J.W., Simonovic, S., St-Hilaire, A. and Whitfield, P.H. (2016) Flood processes in Canada: regional and special aspects. *Canadian Water Resources Journal*, 41(1–2), 7–30. <https://doi.org/10.1080/07011784.2015.1131629>.
- Camarero, J.J., Collado, E., Martínez-de-Aragón, J., De-Miguel, S., Büntgen, U., Martínez-Peña, F., Martín-Pinto, P., Romppanen, T., Salo, K., Oria-de-Rueda, J.A. and Bonet, J.A. (2021) Associations between climate and earlywood and latewood width in boreal and Mediterranean scots pine forests. *Trees*, 35(1), 155–169. <https://doi.org/10.1007/s00468-020-02028-0>.
- Cayford, J.H. and McRae, D.J. (1983) The ecological role of fire in jack pine forests. In: Wein, R.W. and MacLean, D.A. (Eds.) *The role of fire in northern circumpolar ecosystems*, Vol. 18. John Wiley and Sons: New York, pp. 183–199.
- Chen, Y. and She, Y. (2020) Long-term variations of river ice breakup timing across Canada and its response to climate change. *Cold Regions Science and Technology*, 176, 103091. <https://doi.org/10.1016/j.coldregions.2020.103091>.
- Cherry, J.E., Knapp, C., Trainor, S., Ray, A.J., Tedesche, M. and Walker, S. (2017) Planning for climate change impacts on hydropower in the far north. *Hydrology and Earth System Sciences*, 21(1), 133–151. <https://doi.org/10.5194/hess-21-133-2017>.
- Clavet-Gaumont, J., Huard, D., Frigon, A., Koenig, K., Slota, P., Rousseau, A., Klein, I., Thiémonge, N., Houdré, F., Perdikaris, J., Turcotte, R., Lafleur, J. and Larouche, B. (2017) Probable maximum flood in a changing climate: an overview for Canadian basins. *Journal of Hydrology: Regional Studies*, 13(July), 11–25. <https://doi.org/10.1016/j.ejrh.2017.07.003>.

- Cook, E.R. and Kairiukstis, L.A. (1990) *Methods of dendrochronology - applications in the environmental sciences*. Berlin: Springer. <https://doi.org/10.1007/978-94-015-7879-0>.
- Cook, E.R., Krusic, P.J. and Jones, P.D. (2003) Dendroclimatic signals in long tree-ring chronologies from the Himalayas of Nepal. *International Journal of Climatology: A Journal of the Royal Meteorological Society*, 23(7), 707–732. <https://doi.org/10.1002/joc.911>.
- Cook, E.R., Meko, D.M., Stahle, D.W. and Cleaveland, M.K. (1999) Drought reconstructions for the continental United States. *Journal of Climate*, 12(4), 1145–1162. [https://doi.org/10.1175/1520-0442\(1999\)012<1145:DRFTCU>2.0.CO;2](https://doi.org/10.1175/1520-0442(1999)012<1145:DRFTCU>2.0.CO;2).
- Cunderlik, J.M. and Ouarda, T.B. (2009) Trends in the timing and magnitude of floods in Canada. *Journal of Hydrology*, 375(3–4), 471–480. <https://doi.org/10.1016/j.jhydrol.2009.06.050>.
- Dansereau, P.R. and Bergeron, Y. (1993) Fire history in the southern boreal forest of northwestern Quebec. *Canadian Journal of Forest Research*, 23(1), 25–32. <https://doi.org/10.1139/x93-005>.
- Daubois, V., Roy, M., Veillette, J.J. and Ménard, M. (2015) The drainage of Lake Ojibway in glaciolacustrine sediments of northern Ontario and Quebec, Canada. *Boreas*, 44(2), 305–318. <https://doi.org/10.1111/bor.12101>.
- Davi, N.K., Jacoby, G.C. and Wiles, G.C. (2003) Boreal temperature variability inferred from maximum latewood density and tree-ring width data, Wrangell Mountain region, Alaska. *Quaternary Research*, 60(3), 252–262. <https://doi.org/10.1016/j.yqres.2003.07.002>.
- Davis, R.E., Lowit, M.B., Knappenberger, P.C. and Legates, D.R. (1999) A climatology of snowfall-temperature relationships in Canada. *Journal of Geophysical Research: Atmospheres*, 104(D10), 11985–11994. <https://doi.org/10.1029/1999JD900104>.
- Denneler, B., Bergeron, Y. and Bégin, Y. (1999) An attempt to explain the distribution of the tree species composing the riparian forests of Lake Duparquet, southern boreal region of Quebec, Canada. *Canadian Journal of Botany*, 77(12), 1744–1755. <https://doi.org/10.1139/cjb-77-12-1744>.
- Déry, S.J., Stahl, K., Moore, R.D., Whitfield, P.H., Menounos, B. and Burford, J.E. (2009) Detection of runoff timing changes in pluvial, nival, and glacial rivers of western Canada. *Water Resources Research*, 45(4), W04426. <https://doi.org/10.1029/2008WR006975>.
- Despouts, M. and Payette, S. (1992) Recent dynamics of jack pine at its northern distribution limit in northern Quebec. *Canadian Journal of Botany*, 70(6), 1157–1167. <https://doi.org/10.1139/b92-144>.
- Duguay, C.R., Prowse, T.D., Bonsal, B.R., Brown, R.D., Lacroix, M. P. and Ménard, P. (2006) Recent trends in Canadian lake ice cover. *Hydrological Processes: An International Journal*, 20(4), 781–801. <https://doi.org/10.1002/hyp.6131>.
- Estilow, T.W., Young, A.H. and Robinson, D.A. (2015) A long-term northern hemisphere snow cover extent data record for climate studies and monitoring. *Earth System Science Data*, 7(1), 137–142. <https://doi.org/10.5194/essd-7-137-2015>.
- Frank, D. and Esper, J. (2005) Temperature reconstructions and comparisons with instrumental data from a tree-ring network for the European Alps. *International Journal of Climatology: A Journal of the Royal Meteorological Society*, 25(11), 1437–1454. <https://doi.org/10.1002/joc.1210>.
- Fritts, H.C. (1976) *Tree rings and climate*. New York: Academic Press. <https://doi.org/10.1016/B978-0-12-268450-0.X5001-0>.
- Fu, C. and Yao, H. (2015) Trends of ice breakup date in south-central Ontario. *Journal of Geophysical Research*, 120(18), 9220–9236. <https://doi.org/10.1002/2015JD023370>.
- Gaur, A., Gaur, A. and Simonovic, S.P. (2018) Future changes in flood hazards across Canada under a changing climate. *Water*, 10(10), 1441. <https://doi.org/10.3390/w10101441>.
- Gennaretti, F., Arseneault, D., Nicault, A., Perreault, L. and Bégin, Y. (2014) Volcano-induced regime shifts in millennial tree-ring chronologies from northeastern North America. *Proceedings of the National Academy of Sciences*, 111(28), 10077–10082. <https://doi.org/10.1073/pnas.1324220111>.
- Gennaretti, F., Huard, D., Naulier, M., Savard, M., Bégin, C., Arseneault, D. and Guiot, J. (2017) Bayesian multiproxy temperature reconstruction with black spruce ring widths and stable isotopes from the northern Quebec taiga. *Climate Dynamics*, 49(11), 4107–4119. <https://doi.org/10.1007/s00382-017-3565-5>.
- Genries, A., Drobyshev, I. and Bergeron, Y. (2012) Growth–climate response of Jack pine on clay soils in northeastern Canada. *Dendrochronologia*, 30(2), 127–136. <https://doi.org/10.1016/j.dendro.2011.08.005>.
- Ghiggi, G., Humphrey, V., Seneviratne, S.I. and Gudmundsson, L. (2019) GRUN: an observation-based global gridded runoff dataset from 1902 to 2014. *Earth System Science Data*, 11(4), 1655–1674. <https://doi.org/10.5194/essd-11-1655-2019>.
- Girardin, M.P., Bernier, P.Y. and Gauthier, S. (2011) Increasing potential NEP of eastern boreal north American forests constrained by decreasing wildfire activity. *Ecosphere*, 2(3), 1–23. <https://doi.org/10.1890/ES10-00159.1>.
- Girardin, M.P. and Tardif, J.C. (2005) Sensitivity of tree growth to the atmospheric vertical profile in the Boreal Plains of Manitoba, Canada. *Canadian Journal of Forest Research*, 35(1), 48–64. <https://doi.org/10.1139/x04-144>.
- Girardin, M.P., Tardif, J.C., Epp, B. and Conciatori, F. (2009) Frequency of cool summers in interior North America over the past three centuries. *Geophysical Research Letters*, 36(7), L07705. <https://doi.org/10.1029/2009GL037242>.
- Girardin, M.P., Tardif, J.C., Flannigan, M.D. and Bergeron, Y. (2006) Synoptic-scale atmospheric circulation and boreal Canada summer drought variability of the past three centuries. *Journal of Climate*, 19(10), 1922–1947. <https://doi.org/10.1175/JCLI3716.1>.
- Girardin, M.P., Tardif, J.C., Flannigan, M.D. and Bergeron, Y. (2006) Synoptic-scale atmospheric circulation and boreal Canada summer drought variability of the past three centuries. *Journal of Climate*, 19(10), 1922–1947. <https://doi.org/10.1175/JCLI3716.1>.
- Griffin, D., Meko, D.M., Touchan, R., Leavitt, S.W. and Woodhouse, C.A. (2011) Latewood chronology development for summer-moisture reconstruction in the US southwest. *Tree-Ring Research*, 67(2), 87–101. <https://doi.org/10.3959/2011-4.1>.
- Griffin, D., Woodhouse, C.A., Meko, D.M., Stahle, D.W., Faulstich, H.L., Carrillo, C., Touchan, R., Castro, C.L. and Leavitt, S.W. (2013) North American monsoon precipitation reconstructed from tree-ring latewood. *Geophysical Research Letters*, 40(5), 954–958. <https://doi.org/10.1002/grl.50184>.
- Guay, C., Minville, M. and Braun, M. (2015) A global portrait of hydrological changes at the 2050 horizon for the province of

- Québec. *Canadian Water Resources Journal/Revue canadienne des ressources hydriques*, 40(3), 285–302. <https://doi.org/10.1080/07011784.2015.1043583>.
- Guiot, J. (1987) Reconstruction of seasonal temperatures in Central Canada since AD 1700 and detection of the 18.6- and 22-year signals. *Climatic Change*, 10(3), 249–268. <https://doi.org/10.1007/BF00143905>.
- Han, W., Xiao, C.D., Dou, T.F. and Ding, M.H. (2018) Changes in the proportion of precipitation occurring as rain in northern Canada during spring–summer from 1979–2015. *Advances in Atmospheric Sciences*, 35(9), 1129–1136. <https://doi.org/10.1007/s00376-018-7226-3>.
- Harris, I., Osborn, T.J., Jones, P. and Lister, D. (2020) Version 4 of the CRU TS monthly high-resolution gridded multivariate climate dataset. *Scientific Data*, 7(1), 1–18. <https://doi.org/10.1038/s41597-020-0453-3>.
- Hidalgo, H.G., Piechota, T.C. and Dracup, J.A. (2000) Alternative principal components regression procedures for dendrohydrologic reconstructions. *Water Resources Research*, 36(11), 3241–3249. <https://doi.org/10.1029/2000WR900097>.
- Hoffer, M. and Tardif, J.C. (2009) False rings in jack pine and black spruce trees from eastern Manitoba as indicators of dry summers. *Canadian Journal of Forest Research*, 39(9), 1722–1736. <https://doi.org/10.1139/X09-088>.
- Hofgaard, A., Tardif, J.C. and Bergeron, Y. (1999) Dendroclimatic response of *Picea mariana* and *Pinus banksiana* along a latitudinal gradient in the eastern Canadian boreal forest. *Canadian Journal of Forest Research*, 29(9), 1333–1346. <https://doi.org/10.1139/x99-073>.
- Holmes, R.L. (1983) Computer-assisted quality control in tree-ring dating and measurement - COFECHA. *Tree-Ring Bulletin*, 43, 69–78.
- Huang, J., Tardif, J.C., Bergeron, Y., Denneler, B., Berninger, F. and Girardin, M.P. (2010) Radial growth response of four dominant boreal tree species to climate along a latitudinal gradient in the eastern Canadian boreal forest. *Global Change Biology*, 16(2), 711–731. <https://doi.org/10.1111/j.1365-2486.2009.01990.x>.
- Jacoby, G.C. and D'Arrigo, R. (1989) Reconstructed northern hemisphere annual temperature since 1671 based on high-latitude tree-ring data from North America. *Climatic Change*, 14(1), 39–59. <https://doi.org/10.1007/BF00140174>.
- Jacoby, G.C., Ivanciu, I.S. and Ulan, L.D. (1988) A 263-year record of summer temperature for northern Quebec reconstructed from tree-ring data and evidence of a major climatic shift in the early 1800's. *Palaeogeography, Palaeoclimatology, Palaeoecology*, 64(1–2), 69–78. [https://doi.org/10.1016/0031-0182\(88\)90143-5](https://doi.org/10.1016/0031-0182(88)90143-5).
- Jeong, D.I. and Sushama, L. (2018) Rain-on-snow events over North America based on two Canadian regional climate models. *Climate Dynamics*, 50(1), 303–316. <https://doi.org/10.1007/s00382-017-3609-x>.
- Jones, N.E., Petreman, I.C. & Schmidt, B.J. (2015): High flows and freshet timing in Canada: Observed trends; Climate Change Research Report CCRR-42, Ontario Ministry of Natural Resources and Forestry, Science and Research Branch, Peterborough. Available at: http://www.climateontario.ca/MNR_Publications/CCRR42.pdf [Accessed 21 June, 2021]
- Kames, S., Tardif, J.C. and Bergeron, Y. (2016) Continuous early-wood vessels chronologies in floodplain ring-porous species can improve dendrohydrological reconstructions of spring high flows and flood levels. *Journal of Hydrology*, 534, 377–389. <https://doi.org/10.1016/j.jhydrol.2016.01.002>.
- Kozłowski, T.T. and Pallardy, S.G. (1997) *Growth control in woody plants*, 1st edition. Elsevier: Academic Press.
- Larsson, L.A. (2003a). CooRecorder: image co-ordinate recording program. Available at: <http://www.cybis.se>
- Larsson, L.A. (2003b). CDendro: Cybis Dendro dating program. Available at: <http://www.cybis.se>
- Lemay, M. and Begin, Y. (2008) Hydroclimatic analysis of an ice-scar tree-ring chronology of a high-boreal lake in northern Québec, Canada. *Hydrology Research*, 39(5–6), 451–464. <https://doi.org/10.2166/nh.2008.003>.
- McCarroll, D., Young, G.H. and Loader, N.J. (2015) Measuring the skill of variance-scaled climate reconstructions and a test for the capture of extremes. *The Holocene*, 25(4), 618–626. <https://doi.org/10.1177/0959683614565956>.
- Meko, D.M. and Baisan, C.H. (2001) Pilot study of latewood-width of conifers as an indicator of variability of summer rainfall in the north American monsoon region. *International Journal of Climatology*, 21, 697–708. <https://doi.org/10.1002/joc.646>.
- Meko, D.M. and Graybill, D.A. (1995) Tree-ring reconstruction of upper Gila River discharge. *Journal of the American Water Resources Association*, 31(4), 605–616. <https://doi.org/10.1111/j.1752-1688.1995.tb03388.x>.
- Miina, J. (2000) Dependence of tree-ring, earlywood and latewood indices of Scots pine and Norway spruce on climatic factors in eastern Finland. *Ecological Modelling*, 132(3), 259–273. [https://doi.org/10.1016/S0304-3800\(00\)00296-9](https://doi.org/10.1016/S0304-3800(00)00296-9).
- Minville, M., Brissette, F. and Leconte, R. (2008) Uncertainty of the impact of climate change on the hydrology of a nordic watershed. *Journal of Hydrology*, 358(1–2), 70–83. <https://doi.org/10.1016/j.jhydrol.2008.05.033>.
- Mongrain, S. (2014) Dates de dégel du lac Duparquet. *Le Grand Héron: Le Journal de Duparquet*, 19(1), 6. Available at: http://duparquet.ao.ca/documents/pages/19_1-juin-2014.pdf [Accessed 21 June, 2021].
- Monk, W.A., Peters, D.L., Allen Curry, R. and Baird, D.J. (2011) Quantifying trends in indicator hydroecological variables for regime-based groups of Canadian rivers. *Hydrological Processes*, 25(19), 3086–3100. <https://doi.org/10.1002/hyp.8137>.
- Mood, B.J., Coulthard, B. and Smith, D.J. (2020) Three hundred years of snowpack variability in southwestern British Columbia reconstructed from tree-rings. *Hydrological Processes*, 34(25), 5123–5133. <https://doi.org/10.1002/hyp.13933>.
- Mortsch, L., Cohen, S. and Koshida, G. (2015) Climate and water availability indicators in Canada: challenges and a way forward. Part II—historic trends. *Canadian Water Resources Journal*, 40(2), 146–159. <https://doi.org/10.1080/07011784.2015.1006024>.
- Mudryk, L., Derksen, C., Howell, S., Laliberté, F., Thackeray, C., Sospedra-Alfonso, R., Vionnet, V., Kushner, P.J. and Brown, R. D. (2018) Canadian snow and sea ice: historical trends and projections. *The Cryosphere*, 12, 1157–1176. <https://doi.org/10.5194/tc-12-1157-2018>.
- Nolin, A.F., Tardif, J.C., Conciatori, F. and Bergeron, Y. (2021a) Spatial coherency of the spring flood signal among major river basins of eastern boreal Canada inferred from flood rings.

- Journal of Hydrology*, 596, 126084. <https://doi.org/10.1016/j.jhydrol.2021.126084>.
- Nolin, A.F., Tardif, J.C., Conciatori, F., Kames, S., Meko, D.M. and Bergeron, Y. (2021b) Multi-century tree-ring anatomical evidence reveals increasing frequency and magnitude of spring discharge and floods in eastern boreal Canada. *Global and Planetary Change*, 199, 103444. <https://doi.org/10.1016/j.gloplacha.2021.103444>.
- Prowse, T.D. and Bonsal, B.R. (2004) Historical trends in river-ice breakup: a review. *Hydrology Research*, 35(4–5), 281–293. <https://doi.org/10.2166/nh.2004.0021>.
- R Core Team. (2021). R: A Language and Environment for Statistical Computing. R Foundation for Statistical Computing, Vienna, Austria. Available at: <https://R-project.org/>
- Rohde, R., Muller, R.A., Jacobsen, R., Muller, E., Perlmutter, S., Rosenfeld, A., Wurtele, J., Groom, D. and Wickham, C. (2013) A new estimate of the average earth surface land temperature spanning 1753 to 2011. *Geoinformatics & Geostatistics: An Overview*, 60(1), 1–6. <https://doi.org/10.4172/2327-4581.1000101>.
- Rossi, S., Anfodillo, T., Čufar, K., Cuny, H.E., Deslauriers, A., Fonti, P., Frank, D., Gričar, J., Gruber, A., King, G.M., Krause, C., Morin, H., Oberhuber, W., Prislán, P. and Rathgeber, C.B. (2013) A meta-analysis of cambium phenology and growth: linear and non-linear patterns in conifers of the northern hemisphere. *Annals of Botany*, 112(9), 1911–1920. <https://doi.org/10.1093/aob/mct243>.
- Rudolph, T.D. and Laidly, P.R. (1990) Jack pine. In: Burns, R.M. and Honkala, B.H. (Eds.) *Sylvics of North America, USDA Forest Service, Agriculture Handbook 654*, Vol. 1 Conifers. Washington: Forest Service, United States Department of Agriculture, pp. 280–293.
- Schweingruber, F.H. (1996) *Tree Rings and Environment: Dendroecology*. Berne: Paul Haupt, p. 609.
- Shamir, E., Meko, D., Touchan, R., Lepley, K.S., Campbell, R., Kaliff, R.N. and Georgakakos, K.P. (2020) Snowpack-and soil water content-related hydrologic indices and their association with radial growth of conifers in the Sierra Nevada, California. *Journal of Geophysical Research: Biogeosciences*, 125(1), e2019JG005331. <https://doi.org/10.1029/2019JG005331>.
- Slivinski, L.C., Compo, G.P., Sardeshmukh, P.D., Whitaker, J.S., McColl, C., Allan, R.J., Brohan, P., Yin, X., Smith, C.A., Spencer, L.J., Vose, R.S., Rohrer, M., Conroy, R.P., Schuster, D.C., Kennedy, J.J., Ashcroft, L., Brönnimann, S., Brunet, M., Camuffo, D., Cornes, R., Cram, T.A., Domínguez-Castro, F., Freeman, J.E., Gergis, J., Hawkins, E., Jones, P.D., Kubota, H., Lee, T.C., Lorrey, A.M., Luterbacher, J., Mock, C.J., Przybylak, R.K., Pudmenzky, C., Slonosky, V.C., Tinz, B., Trewin, B., Wang, X.L., Wilkinson, C., Wood, K. and Wyszyński, P. (2021) An evaluation of the performance of the twentieth century reanalysis version 3. *Journal of Climate*, 34(4), 1417–1438. <https://doi.org/10.1175/JCLI-D-20-0505.1>.
- Slivinski, L.C., Compo, G.P., Whitaker, J.S., Sardeshmukh, P.D., Giese, B.S., McColl, C., Allan, R., Yin, X., Vose, R., Titchner, H., Kennedy, J., Spencer, L.J., Ashcroft, L., Brönnimann, S., Brunet, M., Camuffo, D., Cornes, R., Cram, T. A., Crouthamel, R., Domínguez-Castro, F., Freeman, J.E., Gergis, K., Hawkins, E., Jones, P.D., Jourdain, S., Kaplan, A., Kubota, H., Le Blancq, F., Lee, T.-C., Lorrey, A., Luterbacher, J., Maugeri, M., Mock, C.J., Moore, G.W.K., Przybylak, R., Pudmenzky, C., Reason, C., Slonosky, V.C., Smith, C.A., Tinz, B., Trewin, B., Valente, M.A., Wang, X.L., Wilkinson, C., Wood, K. and Wyszyński, P. (2019) Towards a more reliable historical reanalysis: improvements for version 3 of the twentieth century reanalysis system. *Quarterly Journal of the Royal Meteorological Society*, 145(724), 2876–2908. <https://doi.org/10.1002/qj.3598>.
- Stahle, D.W., Cleaveland, M.K., Grissino-Mayer, H.D., Griffin, R. D., Fye, F.K., Therrell, M.D., Burnett, D.J., Meko, D. and Villanueva Diaz, J. (2009) Cool-and warm-season precipitation reconstructions over western New Mexico. *Journal of Climate*, 22(13), 3729–3750. <https://doi.org/10.1175/2008JCLI2752.1>.
- Tardif, J. (1996) Earlywood, latewood, and total ring width of a ring-porous species (*Fraxinus nigra* Marsh.) in relation to climate and hydrologic factors. In: Dean, J.S., Meko, D.M. and Swetnam, T.W. (Eds.) *Tree Rings, Environment, and Humanities*. Arizona: Radiocarbon University of Arizona, pp. 315–324.
- Tardif, J. and Bergeron, Y. (1992) Analyse écologique des peuplements de frêne noir (*Fraxinus nigra*) des rives du lac Duparquet, nord-ouest du Québec. *Canadian Journal of Botany*, 70(11), 2294–2302. <https://doi.org/10.1139/b92-285>.
- Tardif, J. and Bergeron, Y. (1997) Ice-flood history reconstructed with tree-rings from the southern boreal forest limit, western Québec. *The Holocene*, 7(3), 291–300. <https://doi.org/10.1177/095968369700700305>.
- Tardif, J. and Bergeron, Y. (1999) Population dynamics of *Fraxinus nigra* in response to flood-level variations, in northwestern Quebec. *Ecological Monographs*, 69(1), 107–125. [https://doi.org/10.1890/0012-9615\(1999\)069\[0107:PDFONI\]2.0.CO;2](https://doi.org/10.1890/0012-9615(1999)069[0107:PDFONI]2.0.CO;2).
- Tardif, J.C., Conciatori, F. and Bergeron, Y. (2001) Comparative analysis of the climatic response of seven boreal tree species from northwestern Québec. *Tree-Ring Research*, 57(2), 169–181. <http://hdl.handle.net/10150/263000>.
- Tardif, J.C., Girardin, M.P. and Conciatori, F. (2011) Light rings as bioindicators of climate change in interior North America. *Global and Planetary Change*, 79(1–2), 134–144. <https://doi.org/10.1016/j.gloplacha.2011.09.001>.
- Therrell, M.D., Stahle, D.W., Cleaveland, M.K. and Villanueva-Diaz, J. (2002) Warm season tree growth and precipitation over Mexico. *Journal of Geophysical Research: Atmospheres*, 107(D14), ACL-6. <https://doi.org/10.1029/2001JD000851>.
- Touchan, R., Black, B., Shamir, E., Hughes, M.K. and Meko, D. M. (2021) A multimillennial snow water equivalent reconstruction from giant sequoia tree rings. *Climate Dynamics*, 56(5), 1507–1518. <https://doi.org/10.1007/s00382-020-05548-0>.
- Trouet, V. and Van Oldenborgh, G.J. (2013) KNMI climate explorer: a web-based research tool for high-resolution paleoclimatology. *Tree-Ring Research*, 69(1), 3–13. <https://doi.org/10.3959/1536-1098-69.1.3>.
- Viau, A.E. and Gajewski, K. (2009) Reconstructing millennial-scale, regional paleoclimates of boreal Canada during the Holocene. *Journal of Climate*, 22(2), 316–330. <https://doi.org/10.1175/2008JCLI2342.1>.
- Vincent, L.A., Zhang, X., Brown, R.D., Feng, Y., Mekis, E., Milewska, E.J., Wan, H. and Wang, X.L. (2015) Observed trends in Canada's climate and influence of low frequency variability

- modes. *Journal of Climate*, 28(11), 4545–4560. <https://doi.org/10.1175/JCLI-D-14-00697.1>.
- Vincent, L.A., Zhang, X., Mekis, É., Wan, H. and Bush, E.J. (2018) Changes in Canada's climate: trends in indices based on daily temperature and precipitation data. *Atmosphere-Ocean*, 56(5), 332–349. <https://doi.org/10.1080/07055900.2018.1514579>.
- Wan, H., Zhang, X. and Zwiers, F. (2019) Human influence on Canadian temperatures. *Climate Dynamics*, 52(1), 479–494. <https://doi.org/10.1007/s00382-018-4145-z>.
- Wang, X., Huang, G., Liu, J., Li, Z. and Zhao, S. (2015) Ensemble projections of regional climatic changes over Ontario. *Canada. Journal of Climate*, 28(18), 7327–7346. <https://doi.org/10.1175/JCLI-D-15-0185.1>.
- Wilson, R., Rao, R., Rydval, M., Wood, C., Larsson, L.Å. and Luckman, B.H. (2014) Blue intensity for dendroclimatology: the BC blues: a case study from British Columbia, Canada. *The Holocene*, 24(11), 1428–1438. <https://doi.org/10.1177/0959683614544051>.
- Wood, S.N. (2003) Thin plate regression splines. *Journal of the Royal Statistical Society: Series B (Statistical Methodology)*, 65(1), 95–114. <https://doi.org/10.1111/1467-9868.00374>.
- Wood, S.N. (2017) *Generalized Additive Models: An Introduction With R*, 2nd edition. London: Chapman and Hall/CRC Press.
- Wood, S.N. (2021). Package ‘mgcv’: mixed GAM computation vehicle with automatic smoothness estimation. R package version 1.8-36. Available at: <https://cran.r-project.org/web/packages/mgcv/mgcv.pdf>
- Youngblut, D. and Luckman, B. (2008) Maximum June–July temperatures in the Southwest Yukon over the last 300 years reconstructed from tree rings. *Dendrochronologia*, 25(3), 153–166. <https://doi.org/10.1016/j.dendro.2006.11.004>.
- Zhang, X., Harvey, K.D., Hogg, W.D. and Yuzyk, T.R. (2001a) Trends in Canadian streamflow. *Water Resources Research*, 37(4), 987–998. <https://doi.org/10.1029/2000WR900357>.
- Zhang, X., Hogg, W.D. and Mekis, É. (2001b) Spatial and temporal characteristics of heavy precipitation events over Canada. *Journal of Climate*, 14(9), 1923–1936. [https://doi.org/10.1175/1520-0442\(2001\)014<1923:SATCOH>2.0.CO;2](https://doi.org/10.1175/1520-0442(2001)014<1923:SATCOH>2.0.CO;2).
- Zhang, X., Vincent, L.A., Hogg, W.D. and Niitsoo, A. (2000) Temperature and precipitation trends in Canada during the 20th century. *Atmosphere-Ocean*, 38, 395–429. <https://doi.org/10.1080/07055900.2000.9649654>.
- Zhang, L., Zhao, Y., Hein-Griggs, D. and Ciborowski, J.J. (2018) Projected monthly temperature changes of the Great Lakes Basin. *Environmental Research*, 167, 453–467. <https://doi.org/10.1016/j.envres.2018.08.017>.

SUPPORTING INFORMATION

Additional supporting information may be found in the online version of the article at the publisher's website.

How to cite this article: Nolin, A. F., Girardin, M. P., Tardif, J. C., Guo, X. J., Conciatori, F., & Bergeron, Y. (2022). A 247-year tree-ring reconstruction of spring temperature and relation to spring flooding in eastern boreal Canada. *International Journal of Climatology*, 1–20. <https://doi.org/10.1002/joc.7608>